Next, a cytotoxicity assay against SNK6 was performed with PBMCs derived from three healthy volunteers with various doses of mogamulizumab. This experiment revealed that cell death increased in a mogamulizumab dose-dependent manner and there was a difference in killing activity among individual PBMCs (Fig. 2B). To determine which cell fraction in PBMCs played a major role of cytotoxicity, CD56-, CD3-, and CD19-positive cells were then used as effector cells. The highest percentage of cell death was observed when target cells were incubated with CD56-positive cells, showing that NK cells played a central role (Fig. 2C). These results indicated that mogamulizumab killed CCR4-positive T- and NK cells via ADCC.

Effect of mogamulizumab in a murine xenograft model

Recently, we reported a murine xenograft model using the immunodeficient NOG mouse and the EBV-positive NK-cell lymphoma cell line, SNK6 (37). We used this model to determine the *in vivo* effects of mogamulizumab. After subcutaneous inoculation with SNK6, mogamulizumab and PBMCs from healthy volunteers were administered. Tumor growth was suppressed significantly in the mogamulizumab-treated group versus the control group ($P < 0.05$; Fig. 3A). A representative image of a tumor-bearing mouse is shown in Fig. 3B. H&E staining and EBER *in situ* hybridization showed the extent of the tumor in each mouse (Fig. 3C and D). In the mogamulizumab-treated mouse, the tumor was regressed with vacuolar degeneration. On the other hand, tumor expansion and massive infiltration in the dermis were seen in the control mouse.

CCR4 expression in patients with EBV-associated LPDs

We next examined the expression of CCR4 on EBV-infected cells from 17 patients with various EBV-associated T/NK-LPDs using a flow-FISH assay. For comparison, 4 patients with PTLD were also examined. Characteristics of each patient are summarized in Supplementary Table S1. CCR4 was expressed on EBV-infected T- and NK cells in 5 of 5 hydroa vacciniforme, 2 of 8 CAEBV, and 1 of 4 hemophagocytic lymphohistiocytosis cases. CCR4 was expressed on EBV-infected B-cells in 1 of 4 patients with PTLD. Representative results of the flow-FISH assay are shown in Fig. 4A. In patients with hydroa vacciniforme (patients 1 and 2), TCR$\gamma\delta^+$ V$\delta2^+$ $\gamma\delta$T cells were positive for EBER, and CCR4 was expressed on the EBER-positive cells. However, in patient 8 with NK cell-type CAEBV ($CD3^-CD56^+$) and patient 14 with hemophagocytic lymphohistiocytosis ($CD3^+CD8^+$), the EBER-positive cells did not express CCR4.

The fluorescence peak of CCR4-treated cells was not clearly separated from that of control IgG-treated cells (Fig. 4A). This is likely because the fluorescence signals were weakened under the harsh conditions of the flow-FISH assay (13). To further confirm CCR4 expression, we stained the presumed EBV-infected population with an anti-CCR4 antibody, without *in situ* hybridization. In patient 1, V$\delta2$-positive $\gamma\delta$T cells harbored EBV (Fig. 4A). Expression of CCR4 was clearly recognized in the V$\delta2$-positive fraction (Fig. 4B), confirming CCR4 expression on EBV-infected $\gamma\delta$T cells in the patient.

Effects of mogamulizumab against tumor cells from a patient with hydroa vacciniforme

To examine the effects of mogamulizumab against tumor cells from patients, an *ex vivo* ADCC assay was performed. First, $\gamma\delta$T cells were isolated from patient 2 by magnetic sorting. In this patient, the $\gamma\delta$T cells harbored EBV (Fig. 4A). Next, we confirmed that more than 90% of the isolated cells were positive for TCR$\gamma\delta$, and that these cells expressed CCR4 (Fig. 5A). Then, the $\gamma\delta$T cells were incubated with mogamulizumab and NK cells from either patient 2 or healthy volunteer controls. The $\gamma\delta$T cells were killed by NK cells from the patient in the presence of mogamulizumab (Fig. 5B). Cytotoxicity was also seen when NK cells from healthy controls were used, and the ADCC activity was similar between NK cells from the patient and those from controls.

Discussion

EBV-associated T/NK-LPDs, initially proposed by Kawa and colleagues (44) and subsequently noted by other researchers (8, 10, 11), are prevalent in eastern Asian countries, and are characterized by clonal expansion of EBV-infected T or NK cells. Because EBV-associated T/NK-LPDs are refractory to conventional chemotherapies and have poor prognoses, there is a continuing need for novel, effective treatments. In this study, we clarified that CCR4 was expressed on EBV-positive T and NK cells in EBV-associated T/NK-LPDs. In particular, in hydroa vacciniforme, CCR4 was expressed on EBV-positive $\gamma\delta$T cells in all the (5 of 5) patients tested. Furthermore, the *ex vivo* ADCC assay showed that $\gamma\delta$T cells isolated from a patient with hydroa vacciniforme were killed by mogamulizumab. Importantly, ADCC activity was similar between NK cells from the patient and those from healthy controls, indicating that the patient's NK cells were capable of killing the tumor cells. Taken together with results from *in vitro* experiments and the *in vivo* mouse xenograft model, our results indicate that mogamulizumab has potential as a therapeutic agent for EBV-associated T/NK-LPDs, at least in CCR4-positive cases.

Among the cell lines used here, SNK1, SNK6, and SNT8 originated from ENKL. All three cell lines expressed CCR4. However, Ishida and colleagues reported that CCR4 was expressed in only 3.7% of tissue samples from patients with ENKL (18). In the present study, CCR4 was expressed in only 1 of 6 patients with NK-cell infection. Thus, there was a discrepancy between established cell lines and patient samples. A previous report showed that expression of CCR4 on naïve NK cells was limited but that *ex vivo* culture, in medium supplemented with interleukin-2, enhanced CCR4 expression (30). Thus, CCR4 expression may have been induced in ENKL cells in establishing or maintaining these cell lines.

Hydroa vacciniforme is characterized by recurrent vesiculopapules, usually occurring on sun-exposed areas, and is seen in children and adolescents (45). In some of these patients, systemic symptoms, including fever, wasting, lymphadenopathy, and hepatosplenomegaly, develop and such systemic disease has been defined as "hydroa vacciniforme-like lymphoma" in the fourth WHO classification of tumors of hematopoietic and lymphoid tissues (12). EBV-infected γδT cells infiltrate the superficial dermis and subcutaneous tissue in hydroa vacciniforme (13, 14). If CCR4 expression is seen in γδT cells, what is the role of CCR4 in the pathogenesis of hydroa vacciniforme? CCR4 plays a major role in chemotaxis, and is attracted to its ligands, CCL17 and CCL22, that are largely expressed in the epidermis (46). ATLL frequently involves the skin, and CCR4 expression in ATLL is considered to be closely associated with skin involvement (24). Like ATLL, CCR4 expression on tumor cells may be related to the clinical features of hydroa vacciniforme.

In addition to hydroa vacciniforme, CCR4 was expressed on EBV-infected T cells in some patients with CAEBV and hemophagocytic lymphohistiocytosis, and even on B-cells in a patient with PTLD. Nakayama and colleagues reported that HTLV-1 promoted CCR4 expression via activation of the AP-1 family, especially Fra-2 (47). It is also known that LMP-1, an EBV oncoprotein, activates the AP-1 pathway in nasopharyngeal carcinoma (48). These reports raise the possibility that EBV infection indirectly promotes CCR4 expression. If the CCR4 expression promoted by EBV plays an important role in the pathogenesis of EBV-associated T/NK-LPDs, targeting CCR4 may be an ideal and definitive therapy.

In conclusion, mogamulizumab has potential as a new therapeutic against EBV-associated T/NK-LPDs, particularly against hydroa vacciniforme. Furthermore, this drug may be effective in other types of EBV-associated T/NK-LPDs, if CCR4 expression can be confirmed. In fact, the use of mogamulizumab is now expanding from ATLL to peripheral T-cell lymphoma and cutaneous T-cell lymphoma, which are positive for CCR4 (22, 49). Further studies with larger samples may expand the range of EBV-associated T/NK-LPDs suitable for mogamulizumab therapy.

Disclosure of Potential Conflicts of Interest

H. Kimura reports receiving a research grant from Kyowa Hakko Kirin Co., Ltd. No potential conflicts of interest were disclosed by the other authors.

Authors' Contributions

Conception and design: T. Kanazawa, S. Iwata, H. Kimura
Development of methodology: T. Kanazawa, Y. Hiramatsu, S. Iwata, M. Siddiquey, H. Kimura
Acquisition of data (provided animals, acquired and managed patients, provided facilities, etc.): T. Kanazawa, S. Iwata, M. Suzuki
Analysis and interpretation of data (e.g., statistical analysis, biostatistics, computational analysis): T. Kanazawa, Y. Hiramatsu, Y. Sato, T. Murata
Writing, review, and/or revision of the manuscript: T. Kanazawa, S. Iwata, Y. Ito, T. Murata, H. Kimura
Administrative, technical, or material support (i.e., reporting or organizing data, constructing databases): T. Kanazawa, Y. Hiramatsu, Y. Ito, F. Goshima, T. Murata, H. Kimura
Study supervision: F. Goshima, T. Murata, H. Kimura
Other (*in vivo* experiments): M. Siddiquey

Acknowledgments

The authors thank Syuko Kumagai and Fumiyo Ando for technical support; and Norio Shimizu (Tokyo Medical and Dental University), Tatsuya Tsurumi (Aichi Cancer Institute), and Yasushi Isobe (St. Marianna University) for providing the cell lines.

The authors also thank the following collaborating institutions and their staff for providing the specimens: Aichi Medical University Hospital, Fukushima Medical University, Jichi Medical University School of Medicine, Juntendo Urayasu Hospital, Kawasaki Medical School, Osaka City General Hospital, Osaka City University Hospital, Saitama Red Cross Hospital, Tenri Yorozu Hospital, Tokai University School of Medicine, University of Miyazaki Hospital, and University of the Ryukyus, Faculty of Medicine.

Grant Support

This study was supported by grants from the Ministry of Education, Culture, Sports, Science and Technology of Japan (25293109) and from the 24th General Assembly of the Japanese Association of Medical Sciences.

The costs of publication of this article were defrayed in part by the payment of page charges. This article must therefore be hereby marked *advertisement* in accordance with 18 U.S.C. Section 1734 solely to indicate this fact.

Received March 8, 2014; revised July 3, 2014; accepted July 21, 2014; published OnlineFirst August 12, 2014.

References

1. Cohen JI. Epstein-Barr virus infection. N Engl J Med 2000;343:481–92.
2. Kwong YL. Natural killer-cell malignancies: diagnosis and treatment. Leukemia 2005;19:2186–94.
3. Williams H, Crawford DH. Epstein-Barr virus: the impact of scientific advances on clinical practice. Blood 2006;107:862–9.
4. Longnecker RM, Kieff E, Cohen JI. Epstein-Barr viru. In:Knipe DM, Howley PM, editors. Fields Virology. 6 ed. Philadelphia: Wolters kluwer/Lippincott Williams & Wilkins; 2013. p. 1898–959.
5. Song SY, Kim WS, Ko YH, Kim K, Lee MH, Park K. Aggressive natural killer cell leukemia: clinical features and treatment outcome. Haematologica 2002;87:1343–5.
6. Chan JKC, Quintanilla-Martinez L, Ferry JA, Peh S-C. Extranodal NK/T-cell lymphoma, nasal type. In:Swerdlow SH, Campo E, Harris NL, et al., editors. WHO Classification of Tumours of Haematopoietic and Lymphoid Tissues. 4th ed. Lyon: WHO Press; 2008. p. 285–8.
7. Kawa K, Okamura T, Yagi K, Takeuchi M, Nakayama M, Inoue M. Mosquito allergy and Epstein-Barr virus-associated T/natural killer-cell lymphoproliferative disease. Blood 2001;98:3173–4.
8. Ohshima K, Kimura H, Yoshino T, Kim CW, Ko YH, Lee SS, et al. Proposed categorization of pathological states of EBV-associated T/natural killer-cell lymphoproliferative disorder (LPD) in children and young adults: overlap with chronic active EBV infection and infantile fulminant EBV T-LPD. Pathol Int 2008;58:209–17.
9. Cohen JI, Kimura H, Nakamura S, Ko YH, Jaffe ES. Epstein-Barr virus-associated lymphoproliferative disease in non-immunocompromised hosts: a status report and summary of an international meeting, 8–9 September 2008. Ann Oncol 2009;20:1472–82.
10. Kimura H, Ito Y, Kawabe S, Gotoh K, Takahashi Y, Kojima S, et al. EBV-associated T/NK-cell lymphoproliferative diseases in nonimmunocompromised hosts: prospective analysis of 108 cases. Blood 2012;119:673–86.
11. Ko Y-H, Kim H-J, Oh Y-H, Park G, Lee S-S, Huh J, et al. EBV-associated T and NK cell lymphoproliferative disorders: Consensus report of the 4th Asian Hematopathology Workshop. J Hematopathol 2013;5:319–24.
12. Quintanilla-Martinez L, Kimura H, Jaffe ES. EBV+ T-cell lymphoma of childhood. In:Swerdlow SH, Campo E, Harris NL, et al., editors. WHO

Classification of Tumours of Haematopoietic and Lymphoid Tissues. 4th ed. Lyon: WHO Press; 2008. p. 278–80.
13. Kimura H, Miyake K, Yamauchi Y, Nishiyama K, Iwata S, Iwatsuki K, et al. Identification of Epstein-Barr virus (EBV)-infected lymphocyte subtypes by flow cytometric *in situ* hybridization in EBV-associated lymphoproliferative diseases. J Infect Dis 2009;200:1078–87.
14. Tanaka C, Hasegawa M, Fujimoto M, Iwatsuki K, Yamamoto T, Yamada K, et al. Phenotypic analysis in a case of hydroa vacciniforme-like eruptions associated with chronic active Epstein-Barr virus disease of gammadelta T cells. Br J Dermatol 2012;166:216–8.
15. Cartron G, Watier H, Golay J, Solal-Celigny P. From the bench to the bedside: ways to improve rituximab efficacy. Blood 2004;104:2635–42.
16. Heslop HE. How I treat EBV lymphoproliferation. Blood 2009;114: 4002–8.
17. Ishii T, Ishida T, Utsunomiya A, Inagaki A, Yano H, Komatsu H, et al. Defucosylated humanized anti-CCR4 monoclonal antibody KW-0761 as a novel immunotherapeutic agent for adult T-cell leukemia/lymphoma. Clin Cancer Res 2010;16:1520–31.
18. Ishida T, Iida S, Akatsuka Y, Ishii T, Miyazaki M, Komatsu H, et al. The CC chemokine receptor 4 as a novel specific molecular target for immunotherapy in adult T-Cell leukemia/lymphoma. Clin Cancer Res 2004;10:7529–39.
19. Yano H, Ishida T, Imada K, Sakai T, Ishii T, Inagaki A, et al. Augmentation of antitumour activity of defucosylated chimeric anti-CCR4 monoclonal antibody in SCID mouse model of adult T-cell leukaemia/lymphoma using G-CSF. Br J Haematol 2008;140:586–9.
20. Ito A, Ishida T, Yano H, Inagaki A, Suzuki S, Sato F, et al. Defucosylated anti-CCR4 monoclonal antibody exercises potent ADCC-mediated antitumor effect in the novel tumor-bearing humanized NOD/Shi-scid, *IL-2Rgamma(null) mouse model. Cancer Immunol Immunother* 2009;58:1195–206.
21. Ito A, Ishida T, Utsunomiya A, Sato F, Mori F, Yano H, et al. Defucosylated anti-CCR4 monoclonal antibody exerts potent ADCC against primary ATLL cells mediated by autologous human immune cells in NOD/Shi-scid, IL-2R gamma(null) mice *in vivo*. J Immunol 2009; 183:4782–91.
22. Yamamoto K, Utsunomiya A, Tobinai K, Tsukasaki K, Uike N, Uozumi K, et al. Phase I study of KW-0761, a defucosylated humanized anti-CCR4 antibody, in relapsed patients with adult T-cell leukemia-lymphoma and peripheral T-cell lymphoma. J Clin Oncol 2010;28:1591–8.
23. Ohshima K, Jaffe ES, Kikuchi M. Adult T-cell leukemia/lymphoma. In: Swerdlow SH, Campo E, Harris NL, et al., editors. WHO Classification of Tumours of Haematopoietic and Lymphoid Tissues. 4 ed. Lyon: WHO Press; 2008. p. 281–4.
24. Ishida T, Utsunomiya A, Iida S, Inagaki H, Takatsuka Y, Kusumoto S, et al. Clinical significance of CCR4 expression in adult T-cell leukemia/lymphoma: its close association with skin involvement and unfavorable outcome. Clin Cancer Res 2003;9:3625–34.
25. Yoshie O, Fujisawa R, Nakayama T, Harasawa H, Tago H, Izawa D, et al. Frequent expression of CCR4 in adult T-cell leukemia and human T-cell leukemia virus type 1-transformed T cells. Blood 2002;99:1505–11.
26. Wakugawa M, Nakamura K, Kakinuma T, Onai N, Matsushima K, Tamaki K. CC chemokine receptor 4 expression on peripheral blood $CD4^+$ T cells reflects disease activity of atopic dermatitis. J Invest Dermatol 2001;117:188–96.
27. Maghazachi AA. G protein-coupled receptors in natural killer cells. J Leukoc Biol 2003;74:16–24.
28. Brandes M, Willimann K, Lang AB, Nam KH, Jin C, Brenner MB, et al. Flexible migration program regulates gamma delta T-cell involvement in humoral immunity. Blood 2003;102:3693–701.
29. Yoshie O, Imai T, Nomiyama H. Chemokines in immunity. Adv Immunol 2001;78:57–110.
30. Inngjerdingen M, Damaj B, Maghazachi AA. Expression and regulation of chemokine receptors in human natural killer cells. Blood 2001;97: 367–75.
31. Bromley SK, Mempel TR, Luster AD. Orchestrating the orchestrators: chemokines in control of T cell traffic. Nat Immunol 2008;9:970–80.
32. Zhang Y, Nagata H, Ikeuchi T, Mukai H, Oyoshi MK, Demachi A, et al. Common cytological and cytogenetic features of Epstein-Barr virus (EBV)-positive natural killer (NK) cells and cell lines derived from patients with nasal T/NK-cell lymphomas, chronic active EBV infection and hydroa vacciniforme-like eruptions. Br J Haematol 2003;121: 805–14.
33. Kaplan J, Tilton J, Peterson WD Jr. Identification of T cell lymphoma tumor antigens on human T cell lines. Am J Hematol 1976;1:219–23.
34. Tsuge I, Morishima T, Morita M, Kimura H, Kuzushima K, Matsuoka H. Characterization of Epstein-Barr virus (EBV)-infected natural killer (NK) cell proliferation in patients with severe mosquito allergy; establishment of an IL-2-dependent NK-like cell line. Clin Exp Immunol 1999;115:385–92.
35. Yagita M, Huang CL, Umehara H, Matsuo Y, Tabata R, Miyake M, et al. A novel natural killer cell line (KHYG-1) from a patient with aggressive natural killer cell leukemia carrying a p53 point mutation. Leukemia 2000;14:922–30.
36. Robertson MJ, Cochran KJ, Cameron C, Le JM, Tantravahi R, Ritz J. Characterization of a cell line, NKL, derived from an aggressive human natural killer cell leukemia. Exp Hematol 1996;24:406–15.
37. Murata T, Iwata S, Siddiquey MN, Kanazawa T, Goshima F, Kawashima D, et al. Heat shock protein 90 inhibitors repress latent membrane protein 1 (LMP1) expression and proliferation of *Epstein-Barr virus-positive natural killer cell lymphoma. PLoS ONE* 2013;8:e63566.
38. Swerdlow SH, Webber SA, Chadburn A, Ferry JA. Post transplant lymphoproliferative disorders. In:Swerdlow SH, Campo E, Harris NL, *et al., editors. WHO Classification of Tumours of Haematopoietic and* Lymphoid Tissues. 4th ed. Lyon: IARC Press; 2008. p. 343–9.
39. Henter JI, Horne A, Arico M, Egeler RM, Filipovich AH, Imashuku S, et al. HLH-2004: diagnostic and therapeutic guidelines for hemophagocytic lymphohistiocytosis. *Pediatr Blood Cancer 2007;48:124–31.*
40. Kimura H, Hoshino Y, Kanegane H, Tsuge I, Okamura T, Kawa K, et al. Clinical and virologic characteristics of chronic active Epstein-Barr virus infection. Blood 2001;98:280–6.
41. Okano M, Kawa K, Kimura H, Yachie A, Wakiguchi H, Maeda A, et al. Proposed guidelines for diagnosing chronic active Epstein-Barr virus infection. Am J Hematol 2005;80:64–9.
42. Iwata S, Yano S, Ito Y, Ushijima Y, Gotoh K, Kawada JI, et al. Bortezomib induces apoptosis in T lymphoma cells and natural killer lymphoma cells independent of epstein-barr virus infection. Int J Cancer 2011;129:2263–73.
43. Kawabe S, Ito Y, Gotoh K, Kojima S, Matsumoto K, Kinoshita T, et al. Application of flow cytometric *in situ* hybridization assay to Epstein-Barr Virus (EBV)-associated T/NK lymphoproliferative diseases. Cancer Sci 2012;103:1481–8.
44. Kawa K. Epstein-Barr virus–associated diseases in humans. Int J Hematol 2000;71:108–17.
45. Iwatsuki K, Xu Z, Takata M, Iguchi M, Ohtsuka M, Akiba H, et al. The association of latent Epstein-Barr virus infection with hydroa vacciniforme. Br J Dermatol 1999;140:715–21.
46. Campbell JJ, Haraldsen G, Pan J, Rottman J, Qin S, Ponath P, et al. The chemokine receptor CCR4 in vascular recognition by cutaneous but not intestinal memory T cells. Nature 1999;400:776–80.
47. Nakayama T, Hieshima K, Arao T, Jin Z, Nagakubo D, Shirakawa AK, et al. Aberrant expression of Fra-2 promotes CCR4 expression and cell proliferation in adult T-cell leukemia. Oncogene 2008;27:3221–32.
48. Zheng H, Li LL, Hu DS, Deng XY, Cao Y. Role of Epstein-Barr virus encoded latent membrane protein 1 in the carcinogenesis of nasopharyngeal carcinoma. Cell Mol Immunol 2007;4:185–96.
49. Tobinai K, Takahashi T, Akinaga S. Targeting chemokine receptor CCR4 in adult T-cell leukemia-lymphoma and other T-cell lymphomas. Curr Hematol Malig Rep 2012;7:235–40.

Cancer Therapy: Preclinical

Clinical Cancer Research

mTOR Inhibitors Induce Cell-Cycle Arrest and Inhibit Tumor Growth in Epstein–Barr Virus–Associated T and Natural Killer Cell Lymphoma Cells

Jun-ichi Kawada[1], Yoshinori Ito[1], Seiko Iwata[2], Michio Suzuki[1], Yoshihiko Kawano[1], Tetsuhiro Kanazawa[2], Mohammed Nure Alam Siddiquey[2], and Hiroshi Kimura[2]

Abstract

Purpose: Epstein–Barr virus (EBV) infects B cells, as well as T cells and natural killer (NK) cells, and is associated with T or NK cell lymphoid malignancies. In various tumor cells, mTOR performs an essential function together with Akt with regard to cell growth. We investigated the effects of mTOR inhibitors on EBV-associated T- and NK-cell lymphomas.

Experimental Design: We investigated the Akt/mTOR activation pathway in EBV-positive and -negative T- and NK-cell lines (SNT13, SNT16, Jurkat, SNK6, KAI3, and KHYG1). We evaluated the antitumor effects of mTOR inhibitors (rapamycin and its analogue, CCI-779) against these cell lines in culture and in a murine xenograft model that was established by subcutaneous injection of SNK6 cells into NOG mice.

Results: All EBV-positive and -negative T- and NK-cell lines tested displayed activation of the Akt/mTOR pathway, and treatment with mTOR inhibitors suppressed mTOR activation. The inhibitors induced G_1 cell-cycle arrest and inhibited cell proliferation in T- and NK-cell lines. Overall, T cell lines were more sensitive to rapamycin, but there were no significant differences between EBV-positive and -negative cell lines. Treatment with rapamycin did not affect lytic or latent EBV gene expression. Intraperitoneal treatment with CCI-779 significantly inhibited the growth of established tumors in NOG mice and reduced the EBV load in peripheral blood.

Conclusion: These results suggest that inhibition of mTOR signaling is a promising new strategy for improving treatment of EBV-associated T- and NK-cell lymphoma. *Clin Cancer Res; 20(21); 5412–22. ©2014 AACR.*

Introduction

Epstein–Barr virus (EBV) is a ubiquitous, oncogenic γ-herpes virus that infects up to 95% of the adult population worldwide. EBV primarily infects B cells, but it can also infect T cells and natural killer (NK) cells and has been associated with multiple lymphoid malignancies, including Burkitt lymphoma, diffuse large B-cell lymphoma, Hodgkin lymphoma, posttransplant lymphoproliferative disorders, nasal NK/T-cell lymphoma, hydroa vacciniforme-like lymphoma, aggressive NK cell leukemia, and chronic active EBV disease (1–3). Treatment of EBV-associated lymphoid malignancies often requires cytotoxic chemotherapies that are not always successful. Rituximab, a humanized monoclonal antibody against CD20, targets B-cell–specific surface antigens present on EBV-transformed malignant cells. It has recently been used for the treatment and prophylaxis of B-cell lymphoma and lymphoproliferative disorders (4). However, there is a continuing need for the effective treatment of T- and NK-cell lymphoid malignancies.

The PI3K/Akt signaling pathway is important for the survival and growth of a range of cancers and is an attractive target for anticancer therapy (5–7). An important downstream target of PI3K/Akt is the mTOR, which mediates phosphorylation of p70S6K and 4E-BP, proteins responsible for the translation and expression of D-type cyclins and c-myc (8, 9). By preventing these phosphorylation events, mTOR inhibitors, such as rapamycin and CCI-779 (temsirolimus), downregulate such expression and induce G_1 cell-cycle arrest (10, 11). It has been shown that mTOR inhibitors have significant antitumor activities on various types of cancer, and CCI-779 became the first FDA-approved mTOR-targeted anticancer agent based on a phase III trial in patients with advanced renal cell carcinoma (12).

In vitro infection of B cells with EBV induces permanent growth transformation and this ability to affect cell growth regulation likely contributes to the development of cancer. Many of the viral proteins expressed in transformed cells, including EBV nuclear antigens and latent membrane

[1]Department of Pediatrics, Nagoya University Graduate School of Medicine, Showa-ku, Nagoya, Japan. [2]Department of Virology, Nagoya University Graduate School of Medicine, Showa-ku, Nagoya, Japan.

Note: Supplementary data for this article are available at Clinical Cancer Research Online (http://clincancerres.aacrjournals.org/).

Corresponding Author: Yoshinori Ito, Department of Pediatrics, Nagoya University Graduate School of Medicine, 65 Tsurumai-cho, Showa-ku, Nagoya 466-8550, Japan. Phone: 81-52-744-2294; Fax: 81-52-744-2974; E-mail: yoshi-i@med.nagoya-u.ac.jp

doi: 10.1158/1078-0432.CCR-13-3172

Translational Relevance

Epstein–Barr virus (EBV) infects B cells, as well as T cells and natural killer (NK) cells, and is associated with T or NK cell lymphoid malignancies. Some of these lymphoid malignancies are refractory and resistant to conventional chemotherapy. This study investigated the Akt/mTOR activation pathway in EBV-positive and -negative T and NK lymphoma cell lines and evaluated the antitumor effects of mTOR inhibitors (rapamycin and its analogue, CCI-779). We found that the Akt/mTOR pathway was activated in all of the T- and NK-cell lines tested. Treatment with mTOR inhibitors induced G_1 cell-cycle arrest and inhibited cell proliferation by suppressing mTOR activation in T- and NK-cell lines. Intraperitoneal treatment with CCI-779 significantly inhibited growth of established tumors in NOG mice and reduced the EBV load in peripheral blood. These findings suggest that mTOR is a promising new therapeutic target for patients with EBV-associated T- and NK-cell lymphoma.

proteins, have profound effects on cell growth regulation and are required for EBV latent infection and B-cell transformation (13). Latent membrane protein 1 (LMP1) is considered to be a major oncoprotein of EBV because activation of NF-κB is required for EBV-induced B-cell transformation and inhibition of it rapidly results in cell death (14, 15). On the other hand, Shair and colleagues have shown that LMP1 also activates PI3K/Akt signaling and this pathway could be an effective target for the treatment of EBV-associated B-cell lymphoma (16). It has previously been shown that the PI3K/Akt/mTOR pathway is activated in EBV-associated B-cell lymphoma cells and that rapamycin modulates the cell cycle and inhibits cell growth (17–20). Furthermore, constitutive activation of the mTOR signaling pathway has been demonstrated in tissue samples from EBV-positive posttransplant lymphoproliferative disorders (21). LMP1 is expressed in EBV-associated T- and NK-cell lymphoma, but PI3K/Akt/mTOR pathway activation in these cells has not been confirmed. Loong and colleagues examined the effects of rapamycin in an EBV-positive NK cell lymphoma xenograft model (22). In that study, rapamycin did not show any effects on the tumor growth, but activation of the mTOR pathway was not evaluated.

In the present study, we evaluated the antitumor effects of mTOR inhibitors on EBV-associated T- and NK-cell lines in culture and in a murine xenograft model and found that mTOR inhibitors induce G_1 cell-cycle arrest and inhibit cell proliferation. These findings suggest that inhibition of mTOR signaling is a promising new strategy to improve treatment of EBV-associated T- and NK-cell lymphoma.

Materials and Methods

Cell lines and reagents

Of the cell lines used in the present study, SNT13 and SNT16 are EBV-positive T cell lines, SNK6 and KAI3 are EBV-positive NK cell lines, and Jurkat and KHYG1 are EBV-negative T- and NK-cell lines, respectively (23–25). SNT13, SNT16, SNK6, and KAI3 cells were derived from patients with chronic active EBV disease or nasal NK/T cell lymphoma. MT2 cell line was established from cord mononuclear cells by coculture with adult T-cell leukemia cells and harbors human T-cell-leukemia virus type I. The MT2/rEBV/9-7 and MT2/rEBV/9-9 cell lines were established following infection of MT2 cells with the hygromycin-resistant EBV B95.8 strain (26). The MT2/hyg cell line was transfected with a hygromycin resistance gene. The NKL cell line was derived from a patient with NK cell leukemia, and the TL1 cell line was established from NKL cells infected with an Akata-transfected recombinant EBV strain carrying a neomycin resistance gene (27). Jurkat cells were grown in RPMI-1640 supplemented with 10% heat-inactivated FBS, penicillin, and streptomycin (complete media). Complete media supplemented with 100 U/mL human IL2 were used for SNT13, SNT16, SNK6, KAI3, KHYG1, NKL, and TL1. Complete media supplemented with 0.2 mg/mL hygromycin were used for MT2/hyg, MT2/rEBV/9-7, and MT2/rEBV/9-9. TL1 underwent periodic selection with G418.

Rapamycin (Cell Signaling Technology) and CCI-779 (Sigma) were dissolved in DMSO and ethanol, respectively. The autophagy inhibitor 3-methyladenine (3-MA; Sigma) was dissolved in DMSO.

Immunoblotting

Cells were lysed directly in sample buffer. Equal amounts of protein were subjected to SDS-PAGE, transferred to polyvinylidene difluoride (PVDF) membranes, and incubated with antibody. Antibody against phospho-Akt (Ser473), Akt, phospho-4E-BP1 (Ser65), 4E-BP1, phospho-p70S6K (Thr389), p70S6K, p27Kip1, LC3B, Atg5-Atg12, and caspase-3 (Cell Signaling Technology); β-actin and PARP (Sigma); and retinoblastoma protein (Rb) and CDK2 (BD Pharmingen Biosciences) were used for immunoblots. To compare the amount of each protein, densitometric analysis was performed using ImageJ software version 1.46r (NIH, Bethesda, MD).

Cell numbers and viability

Cells were cultured in 24-well plates at 2×10^5/mL, and cell numbers and viability were assayed by trypan blue exclusion using a Countess automated cell counter (Invitrogen). Experiments were performed at least in triplicate.

Cell proliferation assay

Cell proliferation was measured by MTS assay using CellTiter 96 AQueous One Solution Cell Proliferation Assay reagent (Promega). Briefly, 100 μL of cell suspension and 20 μL of MTS reagent were incubated in a 96-well plate for 1 hour at 37°C, and formazan absorbance was measured at a wavelength of 490 nm. Experiments were performed in triplicate.

Annexin V analysis of apoptosis

Apoptosis was measured using an Annexin V-PE/7-AAD apoptosis assay kit (BD Pharmingen Biosciences) in

accordance with the manufacturer's instructions. Cells were analyzed by flow cytometry, and viable cells were defined as negative for Annexin V-phycoerythrin (PE) and 7-aminoctinomycin D (7-AAD) staining, whereas apoptotic cells were defined as positive for Annexin V-PE and negative for 7-AAD staining.

Cell-cycle assay

Cells were treated with various concentrations of rapamycin or CCI-779 for 24 hours, fixed with 70% ethanol, and then washed with ice-cold PBS. Fixed cells were treated with 10 μg/mL DNase-free RNase and stained with 5 μg/mL propidium iodide (Sigma). Experiments were performed in triplicate.

Real-time RT-PCR

Viral mRNA expression was quantified by RT-PCR, as described previously, using β2-microglobulin as an endogenous control and reference gene for relative quantification (28, 29). Each experiment was performed in triplicate.

Xenograft model

Mice of the NOD/Shi-*scid*/IL-2Rγ^{null} (NOG) strain were obtained from the Central Institute for Experimental Animals (Kawasaki, Japan) and were maintained under specific pathogen-free conditions in the animal facility of Nagoya University (Nagoya, Japan). The Ethics Review Committee of the Institute approved the experimental protocol. SNK6 cells (1×10^6 cells per flank) were suspended in 100 μL and subcutaneously inoculated into the flanks of mice. Mice were randomized to drug-treated or control groups (30). Tumor size was quantified with calipers twice weekly, and peripheral blood was obtained every 2 weeks. DNA was extracted from 200 μL of peripheral blood, and real-time quantitative PCR for EBV DNA was then performed as described previously (31). CCI-779 was prepared as described previously (32). Briefly, a 50 mg/mL stock solution was prepared in 100% ethanol. The drug was diluted in 5.2% Tween-80, 5.2% polyethylene glycol (PEG) to the appropriate final concentration (final concentration of ethanol is 4%). The CCI-779 drug solution (100 μL) was administrated intraperitoneally (i.p.) 3 times a week for 3 weeks (a total of 9 injections).

Immunohistochemistry

Additional mice were humanely killed at day 25 after inoculation and tumors were excised. Formaldehyde-fixed, paraffin-embedded sections (5 μm) were labeled with anti-Ki-67 antibody (Dako) for 32 minutes at 37°C, followed by staining with a biotinylated immunoglobulin antibody. Proliferation index was determined as the percentage of Ki-67–positive cells ± SE per original magnification (×400). A total of 5 fields were examined and counted from tumors of control and treated groups.

Statistical analysis

Statistical analyses of cell proliferation, cell cycle, tumor volume, EBV load, and Ki-67 were performed using Mann–Whitney *U* test. Probability values of <0.05 were considered to be statistically significant.

Results

Rapamycin inhibits mTOR signaling in T- and NK-cell lines

To confirm activation of the mTOR signaling pathway, we examined the status of phospho-p70S6K (Thr389) and phospho-4E-BP1 (Ser65) in an EBV-negative T cell line (Jurkat), EBV-positive T cell lines (SNT13 and SNT16), an EBV-negative NK cell line (KHYG1), and EBV-positive NK cell lines (KAI3 and SNK6). As shown in Fig. 1A, the phosphorylated form of 4E-BP1was detected in all cell lines tested, regardless of EBV status. Phosphorylated p70S6K was not detected in KIA3 but was detected in the other cell lines tested. Treatment of cell lines with rapamycin induced almost complete inhibition of p70S6K phosphorylation at T389 and partial (20%–80%) inhibition of 4E-BP1 phosphorylation at S65, confirming the role of mTOR as their kinase and indicating the sensitivity of these cells to mTOR inhibitors (Fig. 1A and Supplementary Fig. S1A). Treatment of the cell lines with higher concentrations of rapamycin (100 nmol/L) did not show complete inhibition of 4E-BP1 phosphorylation (data not shown). As it has been well documented that mTOR functions downstream of the PI3/Akt pathway (5), we examined the activation of Akt. As shown in Fig. 1A, phosphorylation at S473 was detected in all T cell lines indicating strong activation of Akt. However, phospho-Akt was not detected in NK cell lines. After treatment with rapamycin, a compensatory increase in Akt phosphorylation was observed in 4 of the 6 tested cell lines (SNT16, SNT13, KHYG1, and SNK6).

Inhibition of mTOR signaling by rapamycin suppresses growth of EBV-positive and -negative T- and NK-cell lines

To determine whether T- and NK-cell lines were sensitive to mTOR inhibitors, they were exposed to 10 to 50 nmol/L of rapamycin, and cell counts were determined after 48 and 72 hours. Neither fresh medium nor additional drugs were added during the observation period. As shown in Fig. 1B and C and Supplementary Fig. S2A, we found that growth in 6 T- and NK-cell lines was inhibited by rapamycin in a dose-dependent manner. In all T- and NK-cell lines, inhibition of cell growth by rapamycin was statistically significant at 72 hours at all concentrations. Overall, T cell lines were more sensitive to rapamycin than NK cell lines. In comparison, at the highest concentration (50 nmol/L) of rapamycin, cell growth inhibition of SNT16 cells was significantly higher than in Jurkat cells, whereas there were no significant differences between Jurkat and SNT13 cells. On the other hand, no significant differences were observed among EBV-positive and -negative NK cell lines at concentration of 50 nmol/L (Fig. 1C). The results of cell proliferation assay using MTS are shown in Supplementary Fig. S2B. Treatment with 10 to 50 nmol/L rapamycin for 72 hours inhibited proliferation of all T- and NK-cell lines in a dose-dependent

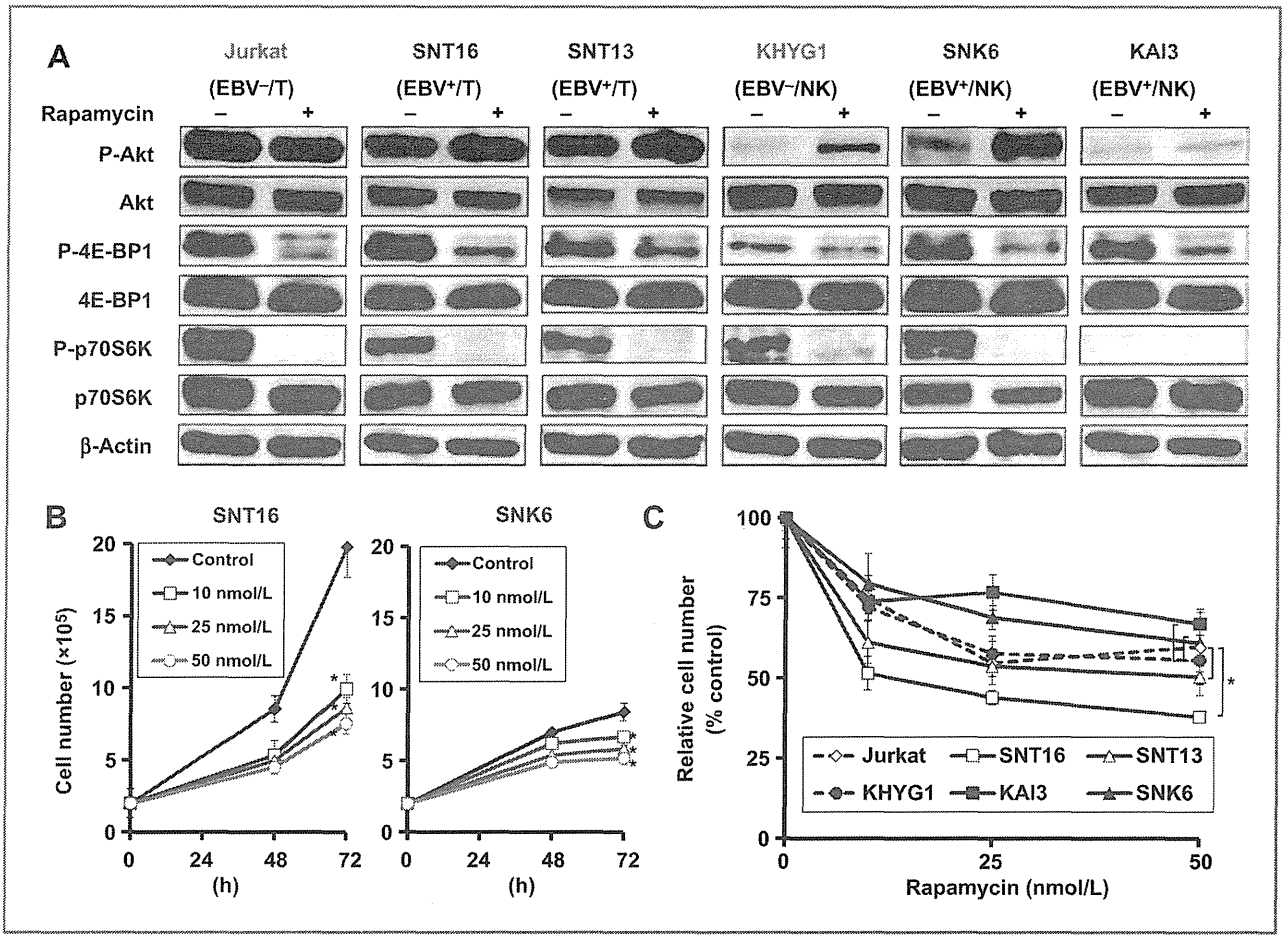

Figure 1. Effects of rapamycin on phosphorylation status of PI3K/Akt/mTOR signaling components and growth in T and NK lymphoma cell lines. A, EBV-negative T cell line (Jurkat), EBV-positive T cell lines (SNT16 and SNT13), an EBV-negative NK cell line (KHYG1), and EBV-positive NK cell lines (SNK6 and KAI3) were treated with 50 nmol/L rapamycin for 1 hour (P-4E-BP1, 4E-BP1, P-p70S6K, and p70S6K) or 24 hours (P-Akt, Akt, and β-actin), and lysates were blotted for the proteins indicated. B, EBV-positive T cell line (SNT16) and an EBV-positive NK cell line (SNK6) were treated with the indicated concentrations of rapamycin, and viable cells were counted using the trypan blue exclusion test. Values are means ± SE of the results from 4 replicate experiments. *, $P < 0.05$, as compared with controls. C, T- and NK-cell lines were treated with the indicated concentrations of rapamycin for 72 hours. Cell number is shown as the ratio of cell numbers in the different treatment groups to DMSO-treated cells. Values are means ± SE of the results from 4 replicate experiments. *, $P < 0.05$.

manner. When compared with untreated cells, inhibition of cell proliferation by rapamycin was statistically significant with 25 and 50 nmol/L in all T- and NK-cell lines. No significant differences were observed among EBV-positive and -negative cell lines. All T- and NK-cell lines tested showed little loss in viability, even at 50 nmol/L rapamycin (data not shown). Treatment of cells with rapamycin over longer periods of time resulted in little or no decrease in viability when compared with untreated cells (Supplementary Fig. S2C).

Rapamycin induces G_1 cell-cycle arrest in T- and NK-cell lines

Induction of cell-cycle arrest by mTOR inhibitors has been reported to inhibit cancer cell growth (10, 11). We examined whether growth inhibition of T and NK cells by rapamycin was a result of cell-cycle arrest. T and NK cells were treated with various concentrations of rapamycin for 24 hours, stained with propidium iodide, and then analyzed using flow cytometry. Significant increases in cells in G_1 phase were observed after treatment with rapamycin in Jurkat, SNT13, SNT16, and KHYG1 cells (Fig. 2A). A similar trend was observed in SNK6 and KAI3 cells, but the increase in cells in the G_1 phase was not significant (Fig. 2A). Consistent with G_1 cell-cycle arrest, reduced levels of corresponding to cell-cycle markers CDK2 and Rb were also observed in all cell lines tested together with increased levels of p27 Kip1 in Jurkat, SNT16, and KHYG1 following treatment with rapamycin for 24 hours (Fig. 2B). Together, these results suggest that rapamycin induced G_1 cell-cycle arrest in T- and NK-cell lines.

CCI-779 induces inhibition of cell proliferation by G_1 cell-cycle arrest in T- and NK-cell lines

We evaluated the effects of CCI-779 on T- and NK-cell lines. CCI-779 is a soluble ester analogue of rapamycin and

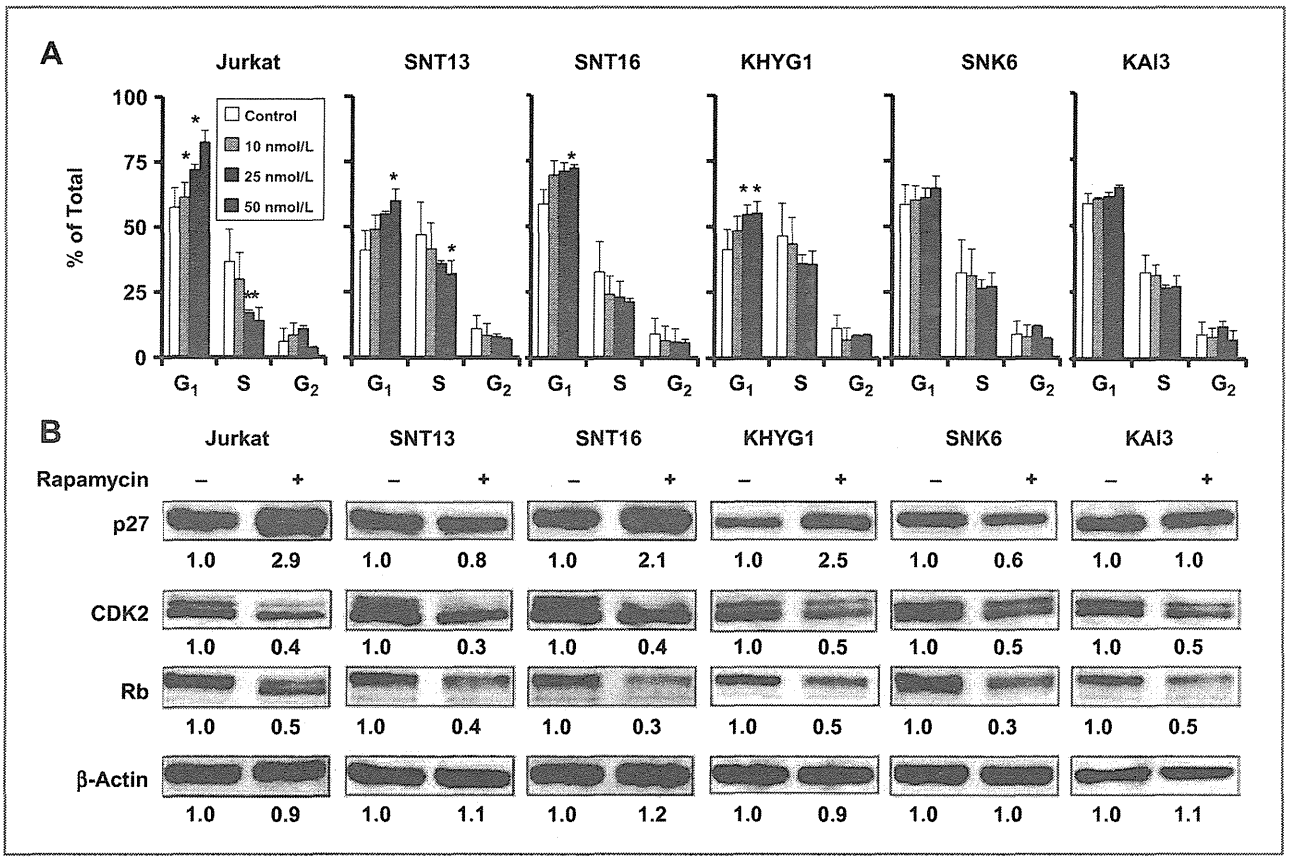

Figure 2. Rapamycin induces G_1 cell-cycle arrest in T- and NK-cell lines. A, T- and NK-cell lines were treated with the indicated concentrations of rapamycin for 24 hours, fixed, and stained with propidium iodide. Cell-cycle profiles were assessed by flow cytometry. Values are means ± SE of 3 independent experiments. *, $P < 0.05$, as compared with controls. B, T- and NK-cell lines were treated with 50 nmol/L rapamycin for 24 hours, and lysates were blotted for the proteins indicated. Numbers below the blots indicate the intensity of each protein relative to untreated cells. Value for untreated cells was set at 1.0.

is more suitable as an intravenous agent than rapamycin (11). Treatment with various concentrations of CCI-779 for 72 hours inhibited proliferation of SNT16 and SNK6 cells in a dose-dependent manner (Supplementary Fig. S3A). As shown in Supplementary Fig. S3B, phosphorylation of both 4E-BP1 and p70S6K was reduced by treatment with CCI-779, suggesting that mTOR activation was inhibited in these cell lines. Cell-cycle analysis showed an increase in G_1 phase cells following treatment with CCI-779, but no decrease in S-phase was observed in SNT16 cells (Supplementary Fig. S3C). Immunoblotting of cycle markers showed reduced levels of Rb in both cell lines and increased levels of p27 Kip1 in SNT16 cells, but no decreases in CDK2 were observed (Supplementary Fig. S3B). These results suggest that CCI-779 induces inhibition of cell proliferation by G_1 cell-cycle arrest, as seen in T- and NK-cell lines treated with rapamycin.

Rapamycin induces little or no apoptosis in T- and NK-cell lines

To evaluate whether rapamycin induces apoptosis, T- and NK-cell lines were treated with 50 nmol/L of rapamycin for 24 and 48 hours, and the cleavage of caspase-3 and PARP was analyzed by immunoblotting. As shown in Fig. 3A and Supplementary Fig. S1B, slightly increased levels of cleaved caspase-3 were detected in SNK6 cells, and slightly increased levels of cleaved PARP were detected in Jurkat, SNK6, and KAI3 cells after 24-hour treatment with rapamycin. Decreased levels of PARP or caspase-3 were not clearly identified. Similar results were seen in T- and NK-cell lines treated with rapamycin for 48 hours (data not shown). Furthermore, apoptosis was analyzed by flow cytometry after Annexin V staining. SNT16 cells treated with rapamycin showed modest increases in apoptotic cells (Annexin V–positive and 7-AAD–negative) when compared with untreated cells (Fig. 3B). Similar results were seen in SNT13 (data not shown). On the other hand, no increase in the number of apoptotic cells was confirmed in SNK6, KAI3, KHYG1, or Jurkat cells (Fig. 3B and data not shown). Taken together, these results suggest that rapamycin induces little or no apoptosis in T- and NK-cell lines.

Effects of rapamycin on autophagy of T- and NK-cell lines

Previous studies have shown that mTOR inhibitors induce autophagy in various cancer cells because the mTOR pathway plays a crucial initiating role in

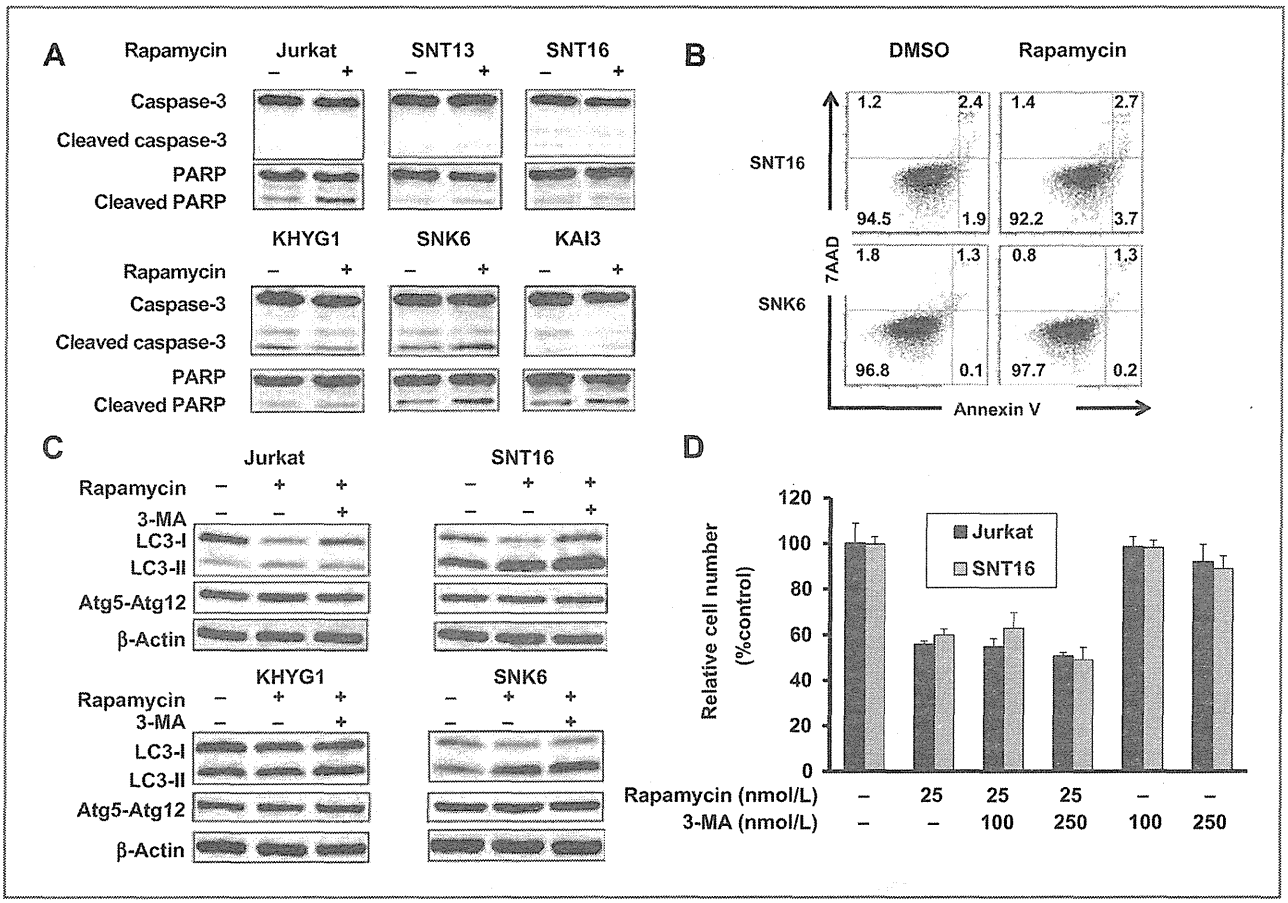

Figure 3. Effects of rapamycin on apoptosis and autophagy in T- and NK-cell lines. A, T- and NK-cell lines were treated with 50 nmol/L rapamycin for 24 hours, and lysates were blotted for caspase-3 and PARP. B, SNT16 and SNK-6 cells were treated with 50 nmol/L rapamycin for 24 hours, and apoptosis was evaluated by Annexin V–7AAD staining using flow cytometry. C, T- and NK-cell lines were treated with 50 nmol/L rapamycin for 24 hours, and lysates were blotted for LC3B and Atg5-Atg12. Cells were also incubated with autophagy inhibitor 3-MA (250 nmol/L) for 1 hour before incubation with rapamycin and immunoblotting. D, Jurkat and SNT16 cells were incubated with or without 3-MA for 1 hour followed by incubation with 25 nmol/L rapamycin for 72 hours. Viable cells were counted using the trypan blue exclusion test. Values are means ± SE of results from triplicate experiments.

autophagy (33, 34). To evaluate whether rapamycin induces autophagy in T- and NK-cell lines, protein expression in LC3-I and LC3-II was examined by immunoblotting. Conversion of LC3-I to the lower migrating form LC3-II has previously been used as an indicator of autophagy. The 3-MA inhibition of LC3-I reduction seems to be true for Jurkat and SNT16 but not for KHYG1, SNT13, or SNK6 when comparing LC3II/LC3I levels from rapamycin and rapamycin + 3-MA samples (Fig. 3C and Supplementary Fig. S1C). On the other hand, treatment with rapamycin did not increase the expression of proautophagic protein Atg5-Atg12 (Fig. 3C). Furthermore, pretreatment with 100 or 250 nmol/L 3-MA did not prevent the rapamycin-induced cell growth inhibition in Jurkat and SNT16 cells (Fig. 3D). Treatment with combination of 3-MA and rapamycin did not show significant differences in the number of cells when compared with rapamycin alone. These results suggest that autophagy may not be a crucial mechanism of rapamycin-induced cell growth inhibition in these cell lines.

Presence of EBV in an NK cell line increases susceptibility to rapamycin

To directly compare the effects of rapamycin in EBV-positive and -negative cell lines, we administered rapamycin to MT-2/hyg, MT2/rEBV/9-7, MT2/rEBV/9-9, NKL, and TL1. As shown in Fig. 4A, the EBV-positive NK cell line (TL1) was more sensitive to rapamycin than its parent cell line (NKL). On the other hand, rapamycin showed almost equal effects on EBV-positive T cell lines (MT2/rEBV/9-7 and MT2/rEBV/9-9) and a control cell line (MT-2/hyg; Fig. 4A). Cell-cycle analysis showed rapamycin-induced G_1 cell-cycle arrest in NKL and TL1 cells, but the effects of rapamycin on the 2 cell lines were similar (Fig. 4B). Significant increases in cells in S-phase were observed in MT2/rEBV/9-7 when compared with MT2/hyg. The difference was not significant between TL1 and NKL cells or between the EBV-positive and -negative T or NK cells. We evaluated the effects of rapamycin on Akt/mTOR pathway activation in these cell lines. Compared with NKL cells, expression of phospho-Akt was upregulated in TL1 cells. On the other hand, phospho-Akt was expressed

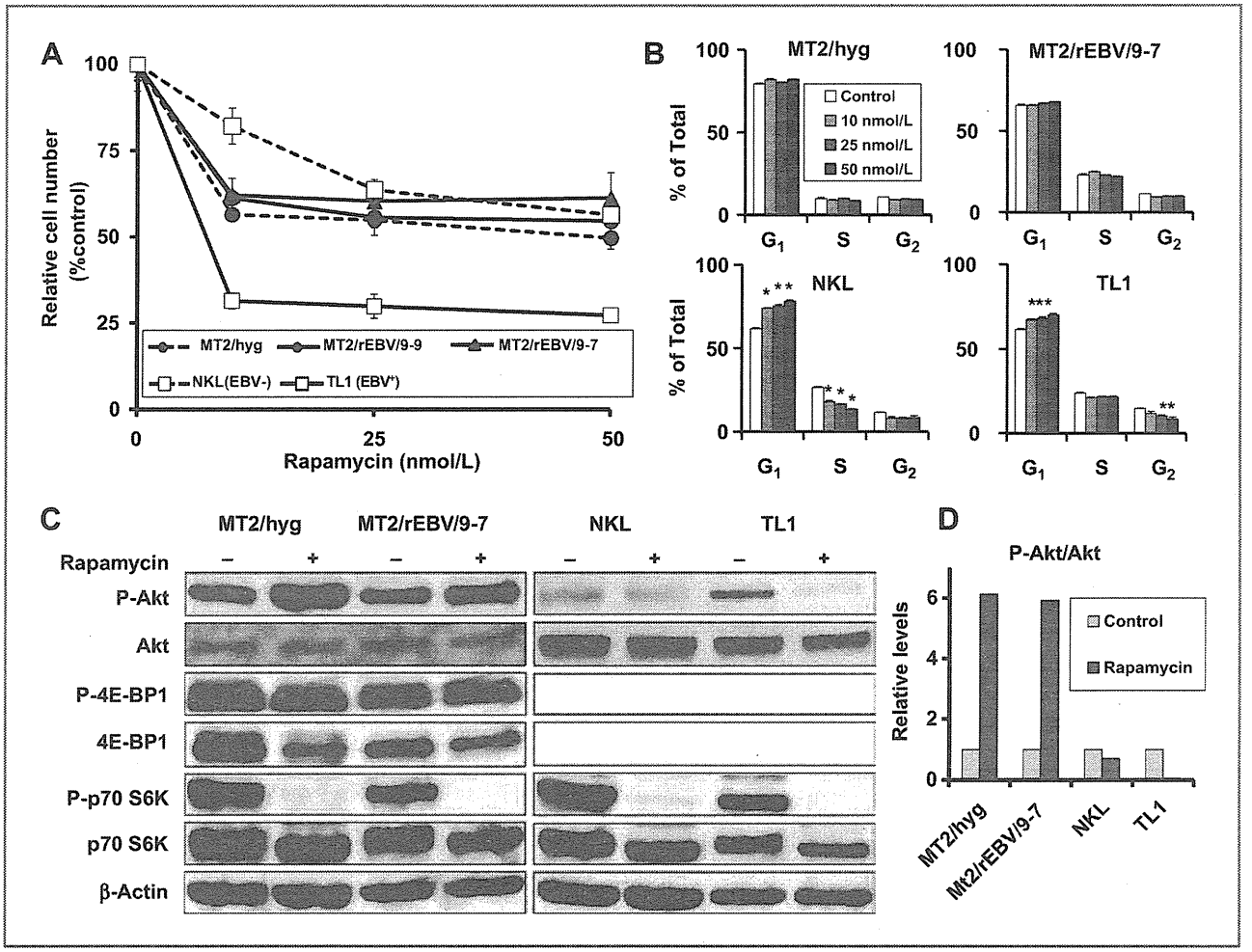

Figure 4. Presence of EBV in an NK cell line increased susceptibility to rapamycin. A, EBV-positive T cell lines (MT2/rEBV/9-7 and MT2/rEBV/9-9) and their parental cell line (MT2/hyg) and an EBV-positive NK cell line (TL1) and its parental cell line (NKL) were treated with the indicated concentrations of rapamycin for 72 hours. Cell number is shown as the ratio of cell numbers in the different treatment groups to DMSO-treated cells. B, T- and NK-cell lines were treated with the indicated concentrations of rapamycin for 24 hours and were fixed and stained with propidium iodide. Cell-cycle profiles were assessed by flow cytometry. Values represent means ± SE of 3 independent experiments. *, $P < 0.05$, as compared with controls. C, T- and NK-cell lines were treated with 20 nmol/L rapamycin for 1 hour (P-4E-BP1, 4E-BP1, P-p70S6K, and p70S6K) or 50 nmol/L rapamycin for 24 hours (P-Akt, Akt, and β-actin), and lysates were blotted for the proteins indicated. D, the ratio of P-Akt to Akt was measured, and the value in untreated (control) cells was set as 1.

in MT-2/hyg and MT2/rEBV/9-7 cells but there were no differences in expression levels (Fig. 4C). Treatment with rapamycin decreased phospho-Akt expression levels in TL1 cells, whereas a compensatory increase in Akt phosphorylation was observed in MT2/hyg and MT2/rEBV/9-7 cells (Fig. 4C and D). Activation of mTOR was confirmed by expression of phospho-p70S6K in these cell lines, and it was suppressed by treatment with rapamycin (Fig. 4C).

Effects of rapamycin on lytic and latent EBV gene expression in T- and NK-cell lines

Expression of the following 8 viral genes was analyzed using real-time RT-PCR: lytic genes encoding BZLF1 and gp350/220; latent genes encoding EBV nuclear antigen (EBNA) 1, EBNA2, latent membrane protein (LMP) 1, LMP2, EBER1, and *Bam*HI-A rightward transcript (BART). Although EBV-positive T- and NK-cell lines are considered to be latency type II, BZLF 1 was detected in all tested cell lines except TL1, and gp350/220 was detected in 2 T cell lines (SNT13 and MT2; Fig. 5). The expression of these lytic genes may come from small fractions of EBV-positive T and NK cells that spontaneously undergo lytic replication. Expression of BZLF1 decreased in rapamycin-treated SNT16 and KAI3 cells, but this effect was not observed in other cell lines (Fig. 5). Expression of 6 latent genes did not differ significantly between rapamycin-treated cells and controls. Representative results for 2 latent genes (those encoding LMP1 and EBER1) are shown in Fig. 5.

CCI-779 inhibited growth of established tumor in NOG mice

We further extended our studies to an *in vivo* xenograft model to validate the significance of our *in vitro* findings. Because of the poor solubility of rapamycin, we used a

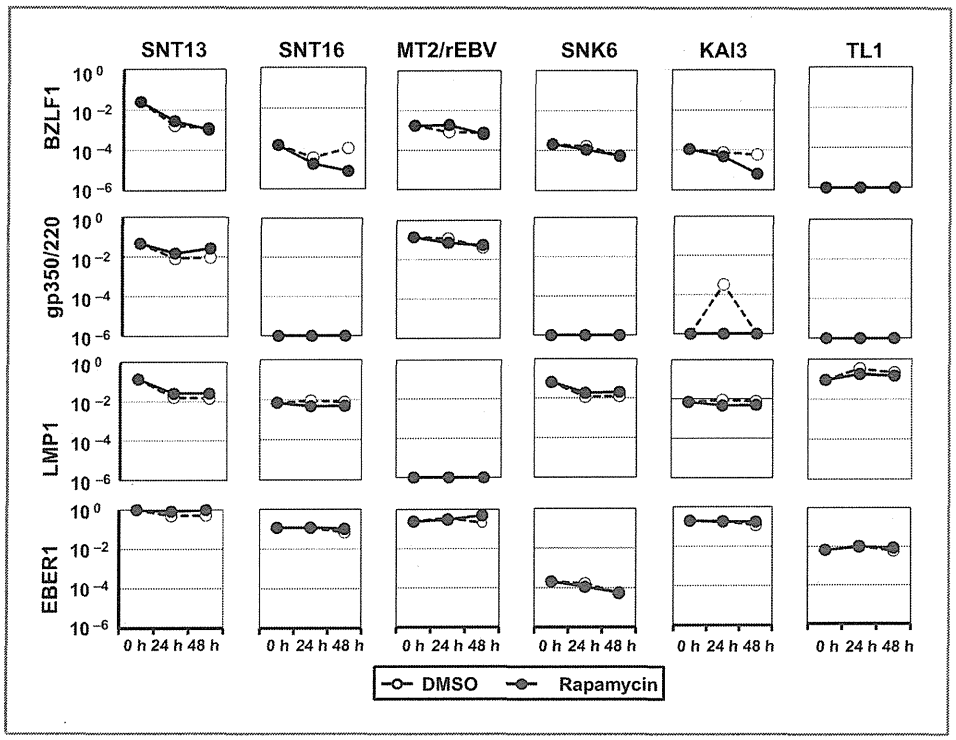

Figure 5. Effects of rapamycin treatment on expression of EBV-encoded genes. EBV-positive T cell lines (SNT13, SNT16, and MT2/rEBV/9-7) and EBV-positive NK cell lines (SNK6, KAI3, and TL1) were treated with 50 nmol/L rapamycin and harvested at 0, 24, and 48 hours to evaluate gene expression using real-time RT-PCR. *BZLF1* is an immediate early gene and *gp350/220* is a late gene. LMP1 and EBER1 are latent genes. β2-Microglobulin was used as an internal control and reference gene for relative quantification and assigned an arbitrary value of 1 (10^0).

water-soluble ester derivative of rapamycin, CCI-779, for treatment of the xenograft model. Subcutaneous inoculation of SNK6 cells into NOG mice resulted in tumor formation at the site of injection in all mice. Four days after the inoculation of SNK6 cells, mice were treated with CCI-779 (10 mg/kg, i.p.) for 3 weeks. Mice generally tolerated CCI-779 with no apparent toxicity throughout the experiment. Figure 6A demonstrates a significant antitumor effect of CCI-779 on tumor growth that was evident 10 days after the start of treatment. Progressive tumor growth was prevented during treatment with CCI-779, and tumor growth after treatment was suppressed for approximately 2 weeks. Subsequently, progressive tumor growth was renewed, but the tumor volume in CCI-779–treated mice was significantly smaller than in the control mice at the end of the study ($2,080 \pm 410$ mm^3 for CCI-779 group and $3,700 \pm 300$ mm^3 for control group; $P < 0.01$). We repeated the NOG mouse experiments to confirm the findings, and the results are shown in Supplementary Fig. S4. Tumor volume in CCI-779-treated -mice was significantly smaller than in control mice from 10 days after the start of treatment until the end of the observation. Peripheral blood was obtained every 2 weeks and EBV load, which may reflect tumor progression, was measured by real-time PCR. EBV load in CCI-779–treated mice was significantly lower than in the control group but increased rapidly after treatment (Fig. 6B). Histologic analyses of tumor explants showed more vacuolar changes in the CCI-779 group (Fig. 6C). To determine whether the observed tumor growth suppression was caused by inhibition of cell proliferation, we performed immunohistochemistry for Ki-67 expression (Fig. 6C). As shown in Fig. 6D, the average proliferation index in 5 randomly selected microscopic fields of CCI-7–treated mice was significantly decreased after 3 weeks of treatment (approximately 30% reduction, $P < 0.01$).

Discussion

The mTOR is a highly conserved serine/threonine kinase and is a central regulator of cell growth, metabolism, and aging (35). Constitutive PI3K/Akt/mTOR activation is critically involved in a variety of cancers and hematologic malignancies (5, 6, 35). Previous studies have shown that the PI3K/Akt/mTOR pathway is activated in EBV-associated B-cell lymphoma, but it is unclear whether this pathway is activated in EBV-associated T- and NK-cell lymphomas (17, 18). This study demonstrated that mTOR is activated in EBV-associated T- and NK-cell lymphoma cells and that mTOR inhibitors induce G_1 cell-cycle arrest and inhibit cell proliferation both *in vitro* and *in vivo*.

Both p70S6K and 4E-BP1 are considered as key mTOR target proteins, and treatment of cell lines with rapamycin or CCI-779 resulted in complete inhibition of p70S6K phosphorylation, whereas inhibition of 4E-BP1 phosphorylation was partial. In some other studies using EBV-positive B cell lines (21) or other cell lines (36, 37), inhibition of 4E-BP1 phosphorylation by rapamycin was partial, whereas inhibition of p70S6K phosphorylation was complete. The reason is uncertain, but activation of survival signaling pathways such as Akt may prevent complete inhibition of 4E-BP1 phosphorylation (37). It has been shown that rapamycin induces Akt activation through an mTOR

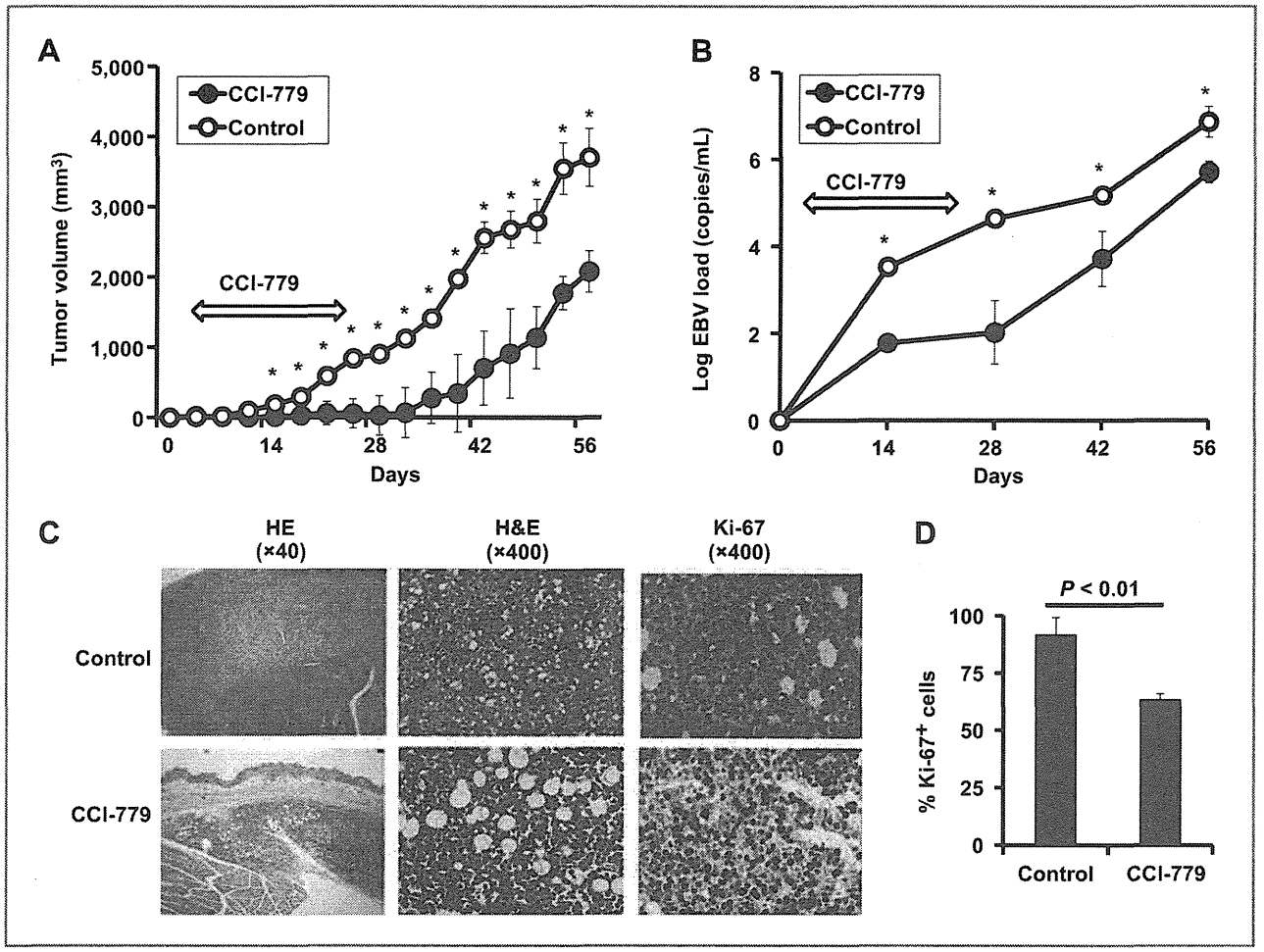

Figure 6. CCI-779 inhibits tumor growth and proliferation in the murine xenograft model. A, CCI-779 inhibits growth of subcutaneous xenograft tumors in NOG mice. SNK6 cells (1×10^6 cells per flank) were subcutaneously inoculated into the flanks of mice. Four days after inoculation of SNK6 cells, mice were treated with CCI-779 (10 mg/kg, i.p.) for 3 weeks, and tumor size was quantified twice weekly. *, $P < 0.05$; $n = 8$ mice for each group. B, peripheral blood was obtained every 2 weeks, and EBV load was measured by real-time PCR. *, $P < 0.05$; $n = 8$ mice for each group. C, representative images of hematoxylin/eosin (HE)-and Ki-67–stained sections of tumors are shown after 3 weeks of treatment with vehicle or CCI-779. D, proliferation was measured by percentage of Ki-67–positive cells. Values are means ± SE of 5 fields in each group.

complex, resulting in the attenuating growth-inhibitory effect of rapamycin (37). As shown in Supplementary Fig. S1A, the increased ratio of phospho -Akt/Akt was marked in KHYG1 and SNK6. On the other hand, small increases in the ratio of phospho-Akt/Akt was observed in SNT13 and SNT16 cells, but not in Jurkat cells. Associations between EBV presence and rapamycin-inducing Akt phosphorylation were inconclusive.

The presence of EBV may have some effect on sensitivity to mTOR inhibitors because LMP1 is known to activate the PI3/Akt pathway, as well as the NF-κB, c-JNK, and p38 MAPK signaling pathways (16, 38). The EBV-positive T- and NK-cell lines used in this study are classified as latency type II and express LMP1. However, there were no marked differences in sensitivity to rapamycin between EBV-positive and -negative cell lines. It is possible that LMP1 has only a small impact on Akt activation in these cell lines because expression of phospho-Akt was similar between EBV-positive and -negative cell lines (Fig. 1A).

T cell lines appeared to be more sensitive to rapamycin and expression of phospho-Akt in T cell lines was higher than in NK cell lines regardless of the presence of EBV. Previous studies have shown that cells with increased Akt activation are more sensitive to mTOR inhibitors (32, 39). The tumor cell origin, rather than the existence of EBV, may have a greater effect on Akt activation and sensitivity to mTOR inhibitors. Interestingly, an artificially EBV-infected NK cell line (TL1) was more sensitive to rapamycin than its parent line (NKL), but there were no differences between EBV-infected T cell lines (MT2/rEBV/9-7 and MT2/rEBV/9-9) and the parental line (MT2/hyg). These differences could be explained by Akt activation, as expression of phospho-Akt was increased in TL1 cells, but not in MT2/rEBV/9-7 cells when compared with the parental lines. Furthermore, LMP1 mRNA was detected in TL1 cells but

not in MT2/rEBV/9-7 cells (Fig. 5). LMP1-induced PI3K/Akt activation might have some impact on dysregulation of mTOR and sensitivity to mTOR inhibitors but further studies are required.

We established a murine xenograft model of EBV-associated NK cell lymphoma and demonstrated tumor growth suppression by CCI-779 *in vivo*. The results of this study showed that T cell lines were more sensitive to rapamycin *in vitro*, but unfortunately, the xenograft model of T-cell lymphoma could not be established. When compared with SNK6 cells, SNT13 and SNT16 cells were more dependent on IL2 for their growth *in vitro* (data not shown). High dependency on IL2 for cell growth might explain the difficulty in establishing a xenograft model using SNT13 or SNT16 cells. Because rapamycin strongly suppresses IL2-stimulated T-cell proliferation, it has been used as an immunosuppressive agent in posttransplant patients (40). Furthermore, several studies have confirmed the antitumor activity of mTOR inhibitors on T-cell acute lymphoblastic leukemia or T-cell lymphoma (41, 42). Further investigations are required to determine whether mTOR inhibitors have more therapeutic potential with EBV-associated T-cell lymphoma than NK cell lymphoma.

In the present study, mTOR inhibitors elicited a cytostatic response in T and NK lymphoma cells resulting in G_1 cell-cycle arrest. Consistent with G_1 cell-cycle arrest, diminished CDK2 and Rb expression and increased p27 Kip1 expression were observed. G_1 cell-cycle arrest induced by mTOR inhibitors has been demonstrated in various types of cancers (10, 11). On the other hand, induction of autophagy or apoptosis is also considered to be a crucial antitumor effect of mTOR inhibitors (33, 34, 41–43), although we found that rapamycin had little or no effect on inducing autophagy or apoptosis in this study. Taken together, our results suggest that mTOR inhibitors can reduce cell growth but cannot cause cell death, resulting in a limited effect in T- and NK-cell lymphomas. In the murine xenograft model, tumor growth was completely prevented during treatment with CCI-779, but progressive tumor growth was subsequently renewed, suggesting that single-agent therapy is limited. Because the success of single-agent therapy with mTOR inhibitors in cancer treatment has been modest, their desirable properties have led to trials in combination with other anticancer agents (44). For example, mTOR inhibitors and the proteasome inhibitor bortezomib act synergistically to induce cell death in some types of cancer (45). Furthermore, synergistic effects of mTOR inhibitors in combination with histone deacetylase inhibitors have been shown in renal cell and prostate carcinoma cell lines (46, 47). Recently, we have shown the antitumor activities of bortezomib and the histone deacetylase inhibitor valproic acid on EBV-associated lymphoma cells (15, 48–50). Combinations of these agents and mTOR inhibitors are promising strategies to improve the treatment of EBV-associated T- and NK-cell lymphomas.

Disclosure of Potential Conflicts of Interest

No potential conflicts of interest were disclosed.

Authors' Contributions

Conception and design: J. Kawada, Y. Ito, H. Kimura
Development of methodology: J. Kawada, T. Kanazawa
Acquisition of data (provided animals, acquired and managed patients, provided facilities, etc.): J. Kawada, S. Iwata, M. Suzuki, Y. Kawano, T. Kanazawa
Analysis and interpretation of data (e.g., statistical analysis, biostatistics, computational analysis): J. Kawada, Y. Ito, S. Iwata, Y. Kawano, T. Kanazawa
Writing, review, and/or revision of the manuscript: J. Kawada, Y. Ito, H. Kimura
Study supervision: Y. Ito, H. Kimura
Other (*in vivo* experiments): M.N.A. Siddiquey

Acknowledgments

The authors thank Norio Shimizu (Tokyo Medical and Dental University, Tokyo, Japan) for the SNK6, SNT13, and SNT16 cell lines; Shigeyoshi Fujiwara (National Research Institute for Child Health and Development, Tokyo, Japan) for the MT2/hyg and MT2/rEBV/9-7 cell lines; and Yasushi Isobe (Juntendo University, Tokyo, Japan) for the NKL and TL1 cell lines. The KAI3 and KHYG1 cells were obtained from the Japanese Collection of Research Bioresources (Osaka, Japan).

The costs of publication of this article were defrayed in part by the payment of page charges. This article must therefore be hereby marked *advertisement* in accordance with 18 U.S.C. Section 1734 solely to indicate this fact.

Received November 20, 2013; revised June 23, 2014; accepted July 18, 2014; published OnlineFirst September 10, 2014.

References

1. Cohen JI. Epstein-Barr virus infection. N Engl J Med 2000;343:481–92.
2. Cohen JI, Kimura H, Nakamura S, Ko YH, Jaffe ES. Epstein-Barr virus-associated lymphoproliferative disease in non-immunocompromised hosts: a status report and summary of an international meeting, 8–9 September 2008. Ann Oncol 2009;20:1472–82.
3. Kimura H, Ito Y, Kawabe S, Gotoh K, Takahashi Y, Kojima S, et al. EBV-associated T/NK-cell lymphoproliferative diseases in nonimmunocompromised hosts: prospective analysis of 108 cases. Blood 2012;119:673–86.
4. Heslop HE. How I treat EBV lymphoproliferation. Blood 2009;114:4002–8.
5. Bjornsti MA, Houghton PJ. The TOR pathway: a target for cancer therapy. Nat Rev Cancer 2004;4:335–48.
6. Dutcher JP. Mammalian target of rapamycin inhibition. Clin Cancer Res 2004;10:6382S–7S.
7. Menon S, Manning BD. Common corruption of the mTOR signaling network in human tumors. Oncogene 2008;27 Suppl 2:S43–51.
8. Abraham RT. Identification of TOR signaling complexes: more TORC for the cell growth engine. Cell 2002;111:9–12.
9. Nelsen CJ, Rickheim DG, Tucker MM, Hansen LK, Albrecht JH. Evidence that cyclin D1 mediates both growth and proliferation downstream of TOR in hepatocytes. J Biol Chem 2003;278:3656–63.
10. Kawamata S, Sakaida H, Hori T, Maeda M, Uchiyama T. The upregulation of p27Kip1 by rapamycin results in G1 arrest in exponentially growing T-cell lines. Blood 1998;91:561–9.
11. Rini BI. Temsirolimus, an inhibitor of mammalian target of rapamycin. Clin Cancer Res 2008;14:1286–90.
12. Hudes G, Carducci M, Tomczak P, Dutcher J, Figlin R, Kapoor A, et al. Temsirolimus, interferon alfa, or both for advanced renal-cell carcinoma. N Engl J Med 2007;356:2271–81.
13. Damania B. Oncogenic gamma-herpesviruses: comparison of viral proteins involved in tumorigenesis. Nat Rev Microbiol 2004;2:656–68.
14. Huen DS, Henderson SA, Croom-Carter D, Rowe M. The Epstein-Barr virus latent membrane protein-1 (LMP1) mediates activation of NF-

kappa B and cell surface phenotype via two effector regions in its carboxy-terminal cytoplasmic domain. Oncogene 1995;10:549–60.
15. Zou P, Kawada J, Pesnicak L, Cohen JI. Bortezomib induces apoptosis of Epstein-Barr virus (EBV)-transformed B cells and prolongs survival of mice inoculated with EBV-transformed B cells. J Virol 2007;81: 10029–36.
16. Shair KH, Bendt KM, Edwards RH, Bedford EC, Nielsen JN, Raab-Traub N. EBV latent membrane protein 1 activates Akt, NFkappaB, and Stat3 in B cell lymphomas. PLoS Pathog 2007;3:e166.
17. Wlodarski P, Kasprzycka M, Liu X, Marzec M, Robertson ES, Slupianek A, et al. Activation of mammalian target of rapamycin in transformed B lymphocytes is nutrient dependent but independent of Akt, mitogen-activated protein kinase/extracellular signal-regulated kinase kinase, insulin growth factor-I, and serum. Cancer Res 2005;65:7800–8.
18. Vaysberg M, Balatoni CE, Nepomuceno RR, Krams SM, Martinez OM. Rapamycin inhibits proliferation of Epstein-Barr virus-positive B-cell lymphomas through modulation of cell-cycle protein expression. Transplantation 2007;83:1114–21.
19. Nepomuceno RR, Balatoni CE, Natkunam Y, Snow AL, Krams SM, Martinez OM. Rapamycin inhibits the interleukin 10 signal transduction pathway and the growth of Epstein Barr virus B-cell lymphomas. Cancer Res 2003;63:4472–80.
20. Cen O, Longnecker R. Rapamycin reverses splenomegaly and inhibits tumor development in a transgenic model of Epstein-Barr virus-related Burkitt's lymphoma. Mol Cancer Ther 2011;10:679–86.
21. El-Salem M, Raghunath PN, Marzec M, Wlodarski P, Tsai D, Hsi E, et al. Constitutive activation of mTOR signaling pathway in post-transplant lymphoproliferative disorders. Lab Invest 2007;87:29–39.
22. Loong SL, Hwang JS, Lim ST, Yap SP, Tao M, Chong TW, et al. An Epstein-Barr virus positive natural killer lymphoma xenograft derived for drug testing. Leuk Lymphoma 2008;49:1161–7.
23. Zhang Y, Nagata H, Ikeuchi T, Mukai H, Oyoshi MK, Demachi A, et al. Common cytological and cytogenetic features of Epstein-Barr virus (EBV)-positive natural killer (NK) cells and cell lines derived from patients with nasal T/NK-cell lymphomas, chronic active EBV infection and hydroa vacciniforme-like eruptions. Br J Haematol 2003;121: 805–14.
24. Tsuge I, Morishima T, Morita M, Kimura H, Kuzushima K, Matsuoka H. Characterization of Epstein-Barr virus (EBV)-infected natural killer (NK) cell proliferation in patients with severe mosquito allergy; establishment of an IL-2-dependent NK-like cell line. Clin Exp Immunol 1999;115:385–92.
25. Yagita M, Huang CL, Umehara H, Matsuo Y, Tabata R, Miyake M, et al. A novel natural killer cell line (KHYG-1) from a patient with aggressive natural killer cell leukemia carrying a p53 point mutation. Leukemia 2000;14:922–30.
26. Fujiwara S, Ono Y. Isolation of Epstein-Barr virus-infected clones of the human T-cell line MT-2: use of recombinant viruses with a positive selection marker. J Virol 1995;69:3900–3.
27. Isobe Y, Sugimoto K, Matsuura I, Takada K, Oshimi K. Epstein-Barr virus renders the infected natural killer cell line, NKL resistant to doxorubicin-induced apoptosis. Br J Cancer 2008;99:1816–22.
28. Kubota N, Wada K, Ito Y, Shimoyama Y, Nakamura S, Nishiyama Y, et al. One-step multiplex real-time PCR assay to analyse the latency patterns of Epstein-Barr virus infection. J Virol Methods 2008;147: 26–36.
29. Iwata S, Wada K, Tobita S, Gotoh K, Ito Y, Demachi-Okamura A, et al. Quantitative analysis of Epstein-Barr virus (EBV)-related gene expression in patients with chronic active EBV infection. J Gen Virol 2010;91:42–50.
30. Murata T, Iwata S, Siddiquey MN, Kanazawa T, Goshima F, Kawashima D, et al. Heat shock protein 90 inhibitors repress latent membrane protein 1 (LMP1) expression and proliferation of Epstein-Barr virus-positive natural killer cell lymphoma. PLoS ONE 2013;8:e63566.
31. Kimura H, Morita M, Yabuta Y, Kuzushima K, Kato K, Kojima S, et al. Quantitative analysis of Epstein-Barr virus load by using a real-time PCR assay. J Clin Microbiol 1999;37:132–6.
32. Neshat MS, Mellinghoff IK, Tran C, Stiles B, Thomas G, Petersen R, et al. Enhanced sensitivity of PTEN-deficient tumors to inhibition of FRAP/mTOR. Proc Natl Acad Sci U S A 2001;98:10314–9.
33. Huang S, Yang ZJ, Yu C, Sinicrope FA. Inhibition of mTOR kinase by AZD8055 can antagonize chemotherapy-induced cell death through autophagy induction and down-regulation of p62/sequestosome 1. J Biol Chem 2011;286:40002–12.
34. Tanemura M, Ohmura Y, Deguchi T, Machida T, Tsukamoto R, Wada H, et al. Rapamycin causes upregulation of autophagy and impairs islets function both in vitro and in vivo. Am J Transplant 2012;12:102–14.
35. Dazert E, Hall MN. mTOR signaling in disease. Curr Opin Cell Biol 2011;23:744–55.
36. Sun SY, Rosenberg LM, Wang X, Zhou Z, Yue P, Fu H, et al. Activation of Akt and eIF4E survival pathways by rapamycin-mediated mammalian target of rapamycin inhibition. Cancer Res 2005;65:7052–8.
37. Wang X, Yue P, Kim YA, Fu H, Khuri FR, Sun SY. Enhancing mammalian target of rapamycin (mTOR)-targeted cancer therapy by preventing mTOR/raptor inhibition-initiated, mTOR/rictor-independent Akt activation. Cancer Res 2008;68:7409–18.
38. Mainou BA, Everly DN Jr, Raab-Traub N. Epstein-Barr virus latent membrane protein 1 CTAR1 mediates rodent and human fibroblast transformation through activation of PI3K. Oncogene 2005;24:6917–24.
39. Marinov M, Ziogas A, Pardo OE, Tan LT, Dhillon T, Mauri FA, et al. AKT/mTOR pathway activation and BCL-2 family proteins modulate the sensitivity of human small cell lung cancer cells to RAD001. Clin Cancer Res 2009;15:1277–87.
40. Kahan BD. Efficacy of sirolimus compared with azathioprine for reduction of acute renal allograft rejection: a randomised multicentre study. The Rapamune US Study Group. Lancet 2000;356:194–202.
41. Chiarini F, Grimaldi C, Ricci F, Tazzari PL, Evangelisti C, Ognibene A, et al. Activity of the novel dual phosphatidylinositol 3-kinase/mammalian target of rapamycin inhibitor NVP-BEZ235 against T-cell acute lymphoblastic leukemia. Cancer Res 2010;70:8097–107.
42. Darwiche N, Sinjab A, Abou-Lteif G, Chedid MB, Hermine O, Dbaibo G, et al. Inhibition of mammalian target of rapamycin signaling by everolimus induces senescence in adult T-cell leukemia/lymphoma and apoptosis in peripheral T-cell lymphomas. Int J Cancer 2011;129: 993–1004.
43. Teachey DT, Obzut DA, Cooperman J, Fang J, Carroll M, Choi JK, et al. The mTOR inhibitor CCI-779 induces apoptosis and inhibits growth in preclinical models of primary adult human ALL. Blood 2006;107: 1149–55.
44. Benjamin D, Colombi M, Moroni C, Hall MN. Rapamycin passes the torch: a new generation of mTOR inhibitors. Nat Rev Drug Discov 2011;10:868–80.
45. Wang C, Gao D, Guo K, Kang X, Jiang K, Sun C, et al. Novel synergistic antitumor effects of rapamycin with bortezomib on hepatocellular carcinoma cells and orthotopic tumor model. BMC Cancer 2012;12:166.
46. Mahalingam D, Medina EC, Esquivel JA II, Espitia CM, Smith S, Oberheu K, et al. Vorinostat enhances the activity of temsirolimus in renal cell carcinoma through suppression of survivin levels. Clin Cancer Res 2010;16:141–53.
47. Thelen P, Krahn L, Bremmer F, Strauss A, Brehm R, Loertzer H. Synergistic effects of histone deacetylase inhibitor in combination with mTOR inhibitor in the treatment of prostate carcinoma. Int J Mol Med 2013;31:339–46.
48. Kawada J, Zou P, Mazitschek R, Bradner JE, Cohen JI. Tubacin kills Epstein-Barr virus (EBV)-Burkitt lymphoma cells by inducing reactive oxygen species and EBV lymphoblastoid cells by inducing apoptosis. J Biol Chem 2009;284:17102–9.
49. Iwata S, Yano S, Ito Y, Ushijima Y, Gotoh K, Kawada J, et al. Bortezomib induces apoptosis in T lymphoma cells and natural killer lymphoma cells independent of Epstein-Barr virus infection. Int J Cancer 2011;129:2263–73.
50. Iwata S, Saito T, Ito Y, Kamakura M, Gotoh K, Kawada J, et al. Antitumor activities of valproic acid on Epstein-Barr virus-associated T and natural killer lymphoma cells. Cancer Sci 2012;103:375–81.

Cancer Science
Japanese Cancer Association JCA
Open Access

Anti-tumor effects of suberoylanilide hydroxamic acid on Epstein–Barr virus-associated T cell and natural killer cell lymphoma

Mohammed N.A. Siddiquey,[1] Hikaru Nakagawa,[1] Seiko Iwata,[1] Tetsuhiro Kanazawa,[1] Michio Suzuki,[1,2] Ken-Ichi Imadome,[3] Shigeyoshi Fujiwara,[3] Fumi Goshima,[1] Takayuki Murata[1] and Hiroshi Kimura[1]

Departments of [1]Virology, [2]Pediatrics, Nagoya University Graduate School of Medicine, Nagoya; [3]Department of Infectious Diseases, National Research Institute for Child Health and Development, Tokyo, Japan

Key words

Extranodal NK-T-cell lymphoma, histone deacetylase inhibitor, human herpesvirus 4, hydroxamic acid, SCID mice

Correspondence

Hiroshi Kimura, Department of Virology, Nagoya University Graduate School of Medicine, 65 Tsurumai-cho, Showa-ku, Nagoya 466-8550, Japan.
Tel: +81-52-744-2207; Fax: +81-52-744-2452;
E-mail: hkimura@med.nagoya-u.ac.jp

Funding information

Ministry of Education, Culture, Sports, Science and Technology of Japan (25293109). Ministry of Health, Labour and Welfare of Japan (H24-Nanchi-046).

Received February 26, 2014; Revised March 31, 2014; Accepted April 7, 2014

Cancer Sci **105** (2014) 713–722

doi: 10.1111/cas.12418

The ubiquitous Epstein–Barr virus (EBV) infects not only B cells but also T cells and natural killer (NK) cells and is associated with various lymphoid malignancies. Recent studies have reported that histone deacetylase (HDAC) inhibitors exert anticancer effects against various tumor cells. In the present study, we have evaluated both the *in vitro* and *in vivo* effects of suberoylanilide hydroxamic acid (SAHA), an HDAC inhibitor, on EBV-positive and EBV-negative T and NK lymphoma cells. Several EBV-positive and EBV-negative T and NK cell lines were treated with various concentrations of SAHA. SAHA suppressed the proliferation of T and NK cell lines, although no significant difference was observed between EBV-positive and EBV-negative cell lines. SAHA induced apoptosis and/or cell cycle arrest in several T and NK cell lines. In addition, SAHA increased the expression of EBV-lytic genes and decreased the expression of EBV-latent genes. Next, EBV-positive NK cell lymphoma cells were subcutaneously inoculated into severely immunodeficient NOD/Shi-scid/IL-2Rγnull mice, and then SAHA was administered intraperitoneally. SAHA inhibited tumor progression and metastasis in the murine xenograft model. SAHA displayed a marked suppressive effect against EBV-associated T and NK cell lymphomas through either induction of apoptosis or cell cycle arrest, and may represent an alternative treatment option.

More than 90% of the world population is infected by the Epstein–Barr virus (EBV), which is an oncogenic γ-herpesvirus. Not only B cells but also T cells and natural killer (NK) cells can be infected by EBV, a condition that is associated with various lymphoid malignancies, including Burkitt lymphoma, Hodgkin lymphoma, post-transplant lymphoproliferative disorders, extranodal NK/T cell lymphoma, hydroa vacciniforme-like lymphoma, aggressive NK cell leukemia and chronic active EBV infection.[1,2] The ability of EBV to establish latent infection and induction of the proliferation of infected cells make it the significant causative agent in the pathogenesis of many of these malignancies. Some of these EBV-associated T and NK cell malignancies are refractory to conventional chemotherapies and have poor prognoses.[3] For the treatment and prophylaxis of B cell lymphoma and lymphoproliferative disorders, rituximab, a humanized monoclonal antibody (Ab) against CD20, targets B cell-specific surface antigens and has been used with marked success.[4,5] However, novel approaches to molecular targeted therapy are required to effectively treat T and NK cell malignancies.

Histone deacetylase (HDAC) inhibitors induce acetylation of histones, thus affecting transcription, and selectively induce tumor-suppressive genes. In various cancer cell types, HDAC inhibitors induce differentiation, apoptosis and cell cycle arrest.[6,7] Moreover, with notable tumor specificity, HDAC inhibitors have potent anticancer activities, and some exhibit therapeutic potential through their targeting of epigenetic regulation. Previously, we showed that an HDAC inhibitor, valproic acid, induced apoptosis and cell cycle arrest in EBV-positive T and NK lymphoma cells.[8] However, the suppressive effect of valproic acid in cell lines was modest and was not affected by the presence of EBV.

Suberoylanilide hydroxamic acid (SAHA) is an FDA-approved HDAC inhibitor, and its efficacy has been confirmed by clinical trials for malignant diseases such as non-Hodgkin lymphoma, acute myeloid leukemia, breast cancer and cutaneous T cell lymphoma.[9–12] Micromolar concentrations of SAHA have anticancer effects and a well-established safety profile.[9] Furthermore, recent studies have confirmed that SAHA can induce EBV lytic infection and mediate enhanced cell death in EBV-positive gastric carcinoma and nasopharyngeal carcinoma cells.[13,14] Very recently, a gene expression profile study identified SAHA as an effective drug candidate for NK cell neoplasms, including EBV-positive NK lymphoma.[15] However, no *in vivo* study has evaluated the efficacy of SAHA in EBV-positive T and NK lymphoma cells.

In the present study, we evaluate the antitumor effects of SAHA on EBV-positive and EBV-negative T and NK cell lines

and analyze induction of apoptosis, cell cycle arrest and expression of EBV-encoded genes. To further evaluate the effect of SAHA, an *in vivo* model is necessary. A suitable host for xenotransplantation of human lymphoid cells is the NOD/Shi-*scid*/IL-2Rγ^{null} (NOG) mouse, which is completely immunodeficient and lacks T, B, NK and dendritic cells, as well as macrophages.[16–19] Recently, the proliferation of EBV-positive T and NK cells has been confirmed by the xenotransplantation of human peripheral blood mononuclear cells (PBMC) to the NOG mouse.[20] Instead of human PBMC, we applied the xenograft model to evaluate SAHA using an EBV-positive NK cell line, which is more suitable for the evaluation of drugs.

Materials and Methods

Cell lines. Of the cell lines used, SNT13 and SNT16 are EBV-positive T cell lines,[21] Jurkat is an EBV-negative T cell line,[22] KAI3 and SNK6 are EBV-positive NK cell lines,[21,23] and KHYG1 is an EBV-negative NK cell line.[24] EBV-positive MT2/rEBV/9-7 and MT2/rEBV/9-9 cell lines were established by infection of MT2 cells with the hygromycin-resistant B95-8 strain.[25,26] EBV-negative MT2/hyg/CL2 and MT2/hyg/CL3 cell lines were transfected with a hygromycin-resistant gene. These four cell lines were used to verify the presence/absence of EBV in the T cell lines. Similarly, the EBV-negative NKL cell line was derived from a patient with NK cell leukemia, and the EBV-positive TL1 cell line was established from NKL cells infected with an Akata-transfected recombinant EBV strain containing a neomycin-resistant gene.[27,28] TL1 and NKL were used to verify the presence/absence of EBV in the NK cell lines. The characteristics of each cell line are summarized in Table 1.

Jurkat cells were cultured in RPMI 1640 medium supplemented with 10% FBS, penicillin, streptomycin and glutamine (complete medium). SNT13, SNT16, KAI3, SNK6, KHYG1, TL1 and NKL cells were grown in complete medium supplemented with 100 U/mL human interleukin-2 (IL-2). MT2/rEBV/9-7, MT2/rEBV/9-9, MT2/hyg/CL2 and MT2/hyg/CL3 cells were grown in complete medium supplemented with 0.2 mg/mL hygromycin. For xenotransplantation, the SNK6 cell line was grown in complete medium supplemented with human serum and 700 U/mL of human IL-2. All cultures were maintained at 37°C in 5% CO_2.

Cell viability. Suberoylanilide hydroxamic acid (Cayman Chemicals, Ann Arbor, MI, USA) was dissolved in DMSO. Each cell line (2×10^5 cells per mL) was cultured in 24-well plates. Human PBMC were isolated from healthy volunteers using Ficoll–Paque (GE Heathcare AB BioSciences, Uppsala, Sweden) gradient centrifugation, and 5×10^5 PBMC per mL were cultured in 24-well plates. Cells were treated with various concentrations of SAHA for 96 h. The cell number and viability were quantified by trypan blue exclusion. Viability was calculated as the percentage of viable SAHA-treated cells versus DMSO-treated cells. These experiments were performed in triplicate, and the results were expressed as mean values with SEM.

Table 1. Characteristics of the cell lines

Name	Cell type	EBV	Cell origin
SNT13	T	+	Chronic active EBV infection
SNT16	T	+	Chronic active EBV infection
Jurkat	T	–	Acute T lymphoblastic leukemia
KAI3	NK	+	Chronic active EBV infection
SNK6	NK	+	Extranodal NK/T cell lymphoma
KHYG1	NK	–	Aggressive NK cell leukemia
MT2/rEBV/9-7	T	+	MT2 cell line
MT2/rEBV/9-9	T	+	MT2 cell line
MT2/hyg/CL2	T	–	MT2 cell line
MT2/hyg/CL3	T	–	MT2 cell line
TL1	NK	+	NKL cell line
NKL	NK	–	NK-cell leukemia

EBV, Epstein–Barr virus; NK, natural killer.

Apoptosis assay by flow cytometry. Apoptosis was measured by flow cytometry using an annexin V-PE/7-AAD apoptosis assay kit (BD Pharmingen Biosciences, San Diego, CA, USA) according to the manufacturer's protocol.[29] Briefly, 2×10^5 cells were treated with SAHA for 24 h, incubated with annexin V-PE and 7-AAD for 15 min, and then analyzed by flow cytometry. Stained cells were analyzed using the FACSCantoII flow cytometer and the FlowJo software (Tree Star, Ashland, OR, USA).

Immunoblotting. After 24 and 48 h of treatment with various concentrations of SAHA, cell pellets were lysed directly in SDS sample buffer (50 mM Tris-HCl [pH 6.8], 2% SDS, 10% glycerol, 6% 2-mercaptoethanol and 0.0025% bromophenol blue). Cell lysates were separated on 10% acrylamide gels by SDS-PAGE, transferred to PVDF membranes, and immunoblotted with Abs. Abs were used against acetyl-histone H3 (Cell Signaling, Boston, MA, USA), poly (ADP-ribose) polymerase (PARP; Sigma, St. Louis, MO, USA), latent membrane protein (LMP) 1 (S12; BD Biosciences, San Jose, CA, USA),[30] EBV nuclear antigen (EBNA) 1[31] and β-actin (Sigma).

Cell cycle assay. Cells were treated with various concentrations of SAHA for 48 h and fixed with 70% ethanol. Fixed cells were treated with DNase-free RNase, stained with propidium iodide (Sigma) for 15 min, and analyzed by flow cytometry. Stained cells were analyzed using a FACSCalibur (Becton Dickinson, San Jose, CA, USA) flow cytometer and the ModFit LT software (Verity Software House, Topsham, ME, USA).

RT-PCR assay. RNA was extracted using the QIAmp RNeasy Mini Kit (Qiagen, Hilden, Germany), and contaminating DNA was removed by on-column DNase digestion using the RNase-free DNase Set (Qiagen). Viral mRNA expression was quantified by one-step multiplex real-time RT-PCR using the Mx3000P real-time PCR system (Stratagene, La Jolla, CA, USA) as described previously.[32,33] β2-Microglobulin was used as an endogenous control and reference gene for relative quantification.[34] Each experiment was performed in triplicate and was shown as the mean of three samples with the SEM.

Xenograft model using the NOG mouse. Female 6-week-old or 7-week-old NOG mice were obtained from the Central Institute of Experimental Animals, Kawasaki, Japan, and maintained under specific pathogen-free conditions by the approval and guidelines of the Nagoya University Experimentation Animal Committee. On day 0, 1×10^6 SNK6 cells were inoculated subcutaneously as described previously.[35] Each day from days 4 to 28, the mice were treated i.p. with 100 mg/kg SAHA or DMSO (control). Tumor volume was quantified using calipers twice per week and calculated using the following formula: $\pi \times$ short axis $\times$ long axis $\times$ height/6. On day 30, mice were killed, and the tumor and organs were excised. RNA was extracted from the tumor and subjected to real-time RT-PCR to quantify viral gene expression. Peripheral blood was collected, and plasma was separated. DNA was extracted from the plasma and quantified by quantitative real-time PCR.[36]

The Mann–Whitney *U*-test was used to compare tumor volumes, viral mRNA expression and quantity of EBV-DNA. *P*-values <0.05 were deemed to indicate statistical significance.

Epstein–Barr virus-encoded small RNA *in situ* hybridization. Formalin (20%)-fixed and sucrose (0.1%)-fixed tissues were sectioned into 10-μm slices and treated with 1:10 diluted proteinase K. The tissues were incubated at room temperature for 30 min, and were then washed with pure water and ethanol (96%). The tissues were stained for Epstein–Barr virus-encoded small RNA (EBER) by *in situ* hybridization (ISH). EBER-ISH was performed using the EBER PNA Probe (Y5200; Dako) and the PNA ISH detection kit (Dako, Glostrup Denmark) according to the manufacturer's protocol.[33]

Results

Effect of suberoylanilide hydroxamic acid on the viability of T and natural killer cell lines. Epstein–Barr virus-positive and EBV-negative T and NK cell lines were cultured with various concentrations of SAHA. SAHA increased acetylated histone H3 levels, confirming that SAHA worked as an HDAC inhibitor (Fig. 1a). SAHA reduced the viability of all treated cell lines in a dose-dependent manner (Fig. 1b). Next, the same six cell lines were treated with 5 μM SAHA and assessed at different time points. The viability of all six cell lines was reduced by treatment with SAHA for 96 h (Fig. 1c). The effects of SAHA did not differ between EBV-positive and EBV-negative cell lines. In addition, to compare its effects on EBV-positive and EBV-negative cell lines, we treated MT2/rEBV/9-7 and MT2/rEBV/9-9 cells (EBV-positive T cell lines), MT2/hyg/CL2 and MT2/hyg/CL3 cells (EBV-negative T cell lines), TL1 cells (EBV-positive NK cell line) and NKL cells (EBV-negative parental NK cell line) with SAHA. SAHA had similar effects on the EBV-positive and EBV-negative cell lines (Fig. 2a). Moreover, human PBMC were treated with SAHA to evaluate the adverse effects. Viability remained >69% at 96 h, indicating the absence of adverse effects (Fig. 2b).

Effects of suberoylanilide hydroxamic acid on apoptosis and the cell cycle of T and natural killer cell lines. To determine whether apoptosis was induced by SAHA in the tested cell lines, early apoptotic cells were quantified by annexin V and 7-AAD staining. SAHA increased early apoptotic cells in the Jurkat, KAI3 and KHYG1 cell lines (Fig. 3a). In other cell lines, the proportions of early apoptotic cells were not increased. Next, the cleavage of PARP was analyzed by immunoblotting. With the exception of the SNT16 cell line, SAHA induced the cleavage of PARP in the five cell lines (Fig. 3b). Next, effects on the cell cycle were investigated. In the SNT16 and KAI3 cell lines, the population of cells in G1 phase was increased, whereas that in G2 phase was increased in the SNK6 cell line (Fig. 4). In Jurkat and KHYG1 cells, the cell cycle assay was indeterminate because of the massive cell death caused by SAHA.

Effects of suberoylanilide hydroxamic acid on Epstein–Barr virus-encoded genes of Epstein–Barr virus-positive T and natural killer cell lines. The expression of eight EBV-related genes, including lytic genes (BZLF1 and gp350/220) and latent genes (EBNA1, EBNA2, LMP1, LMP2, EBER1 and Bam HI-A rightward transcripts [BART]) were analyzed using real-time RT-PCR. In the SNT13, KAI3 and SNK6 cell lines, the

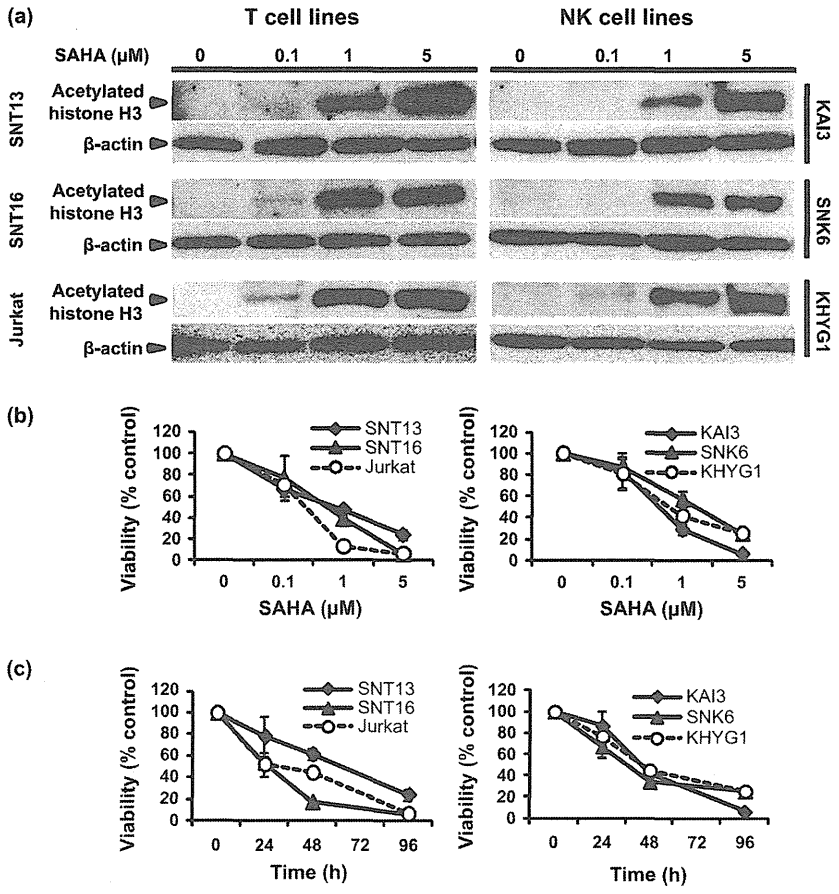

Fig. 1. Suberoylanilide hydroxamic acid (SAHA) inhibits the deacetylation of histone H3 protein and decreases the viability of T and natural killer (NK) cell lines. (a) SNT13, SNT16 (Epstein–Barr virus [EBV]-positive T cell line), Jurkat (EBV-negative T cell line), KAI3, SNK6 (EBV-positive NK cell line) and KHYG1 (EBV-negative NK cell line) cells were treated with the indicated SAHA concentrations for 24 h, and acetylated histone H3 was detected by immunoblotting. β-Actin was used as a loading control. (b) Each cell line was treated with the indicated concentrations of SAHA for 96 h or (c) with 5 μM SAHA for the indicated times. Data are expressed as means ± SEM.

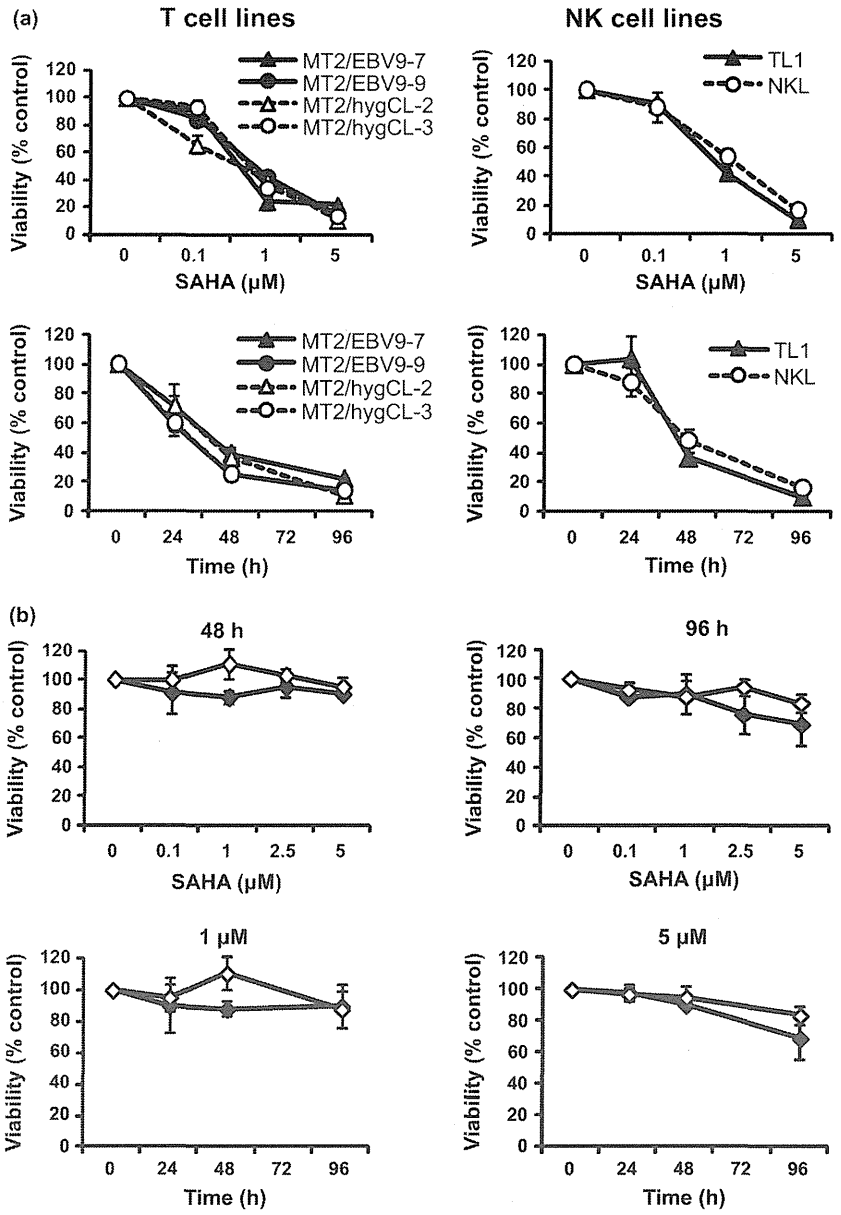

Fig. 2. The effects of suberoylanilide hydroxamic acid (SAHA) do not differ between Epstein–Barr virus (EBV)-positive and EBV-negative cell lines, and SAHA exerts no adverse effects on human peripheral blood mononuclear cells (PBMC). (a) MT2/rEBV/9-7, MT2/rEBV/9-9 (EBV-positive T cell lines), MT2/hyg/CL2, MT2/hyg/CL3 (parental cell lines), TL1 (EBV-positive natural killer [NK] cell line) and NKL (parental cell line) cells were treated with the indicated concentrations of SAHA for 96 h or with 5 μM SAHA for the indicated times. (b) Human PBMC were isolated from two volunteers and treated with the indicated concentrations of SAHA for 48 and 96 h or with 1 and 5 μM SAHA for the indicated times. Data are expressed as means ± SEM.

expression of BZLF1, which is an immediate-early gene in the lytic infection cycle, was increased by SAHA (Fig. 5). However, the expression of the late lytic gene gp350/220 was increased only in the SAHA-treated SNT13 cell line. These results indicated that SAHA induced lytic infection in some EBV-positive T and NK cell lines, although it was abortive. The expression of BZLF1 was decreased in the SAHA-treated SNT16 as time went by, while that in mock-treated SNT16 was also decreased. Of the EBV latent genes tested, the expression of EBNA1, LMP1 and BART was decreased in most of the cell lines, whereas that of LMP2 was increased by SAHA (Fig. 5). Next, the EBNA1 and LMP1 protein levels were determined by immunoblotting. SAHA decreased the EBNA1 protein level in all cell lines, and that of LMP1 in the SNT16, KAI3 and SNK6 cell lines (Fig. 6).

***In vivo* effects of suberoylanilide hydroxamic acid using the mouse xenograft model.** After confirmation of the *in vitro* effect of SAHA, we extended our work to an *in vivo* xenograft model. Initially, we inoculated six T and NK cell lines into immunodeficient NOG mice via various routes. Of the EBV-positive T or NK cell lines used, only the SNK6 cell line was engrafted after subcutaneous or intravenous inoculation (Suppl. Table S1). The Jurkat cell line, which is EBV-negative and IL-2 independent, could also be engrafted, raising the possibility that IL-2 dependency may be associated with the engraftment. We cultured six cell lines with the different concentration of IL-2, and found that SNK6 was less dependent of IL-2 compared with other T/NK cell lines (Suppl. Fig. S1). We considered that the independency of IL-2 can explain the success of engraftment, at least partially. Because evaluation of the former was easier, the subcutaneous model was used in subsequent experiments.

We subcutaneously inoculated 1×10^6 SNK6 cells into NOG mice. All of the mice developed tumors at the site of inoculation. Four days after the inoculation, mice were treated with SAHA daily up to day 28. The treated mice normally

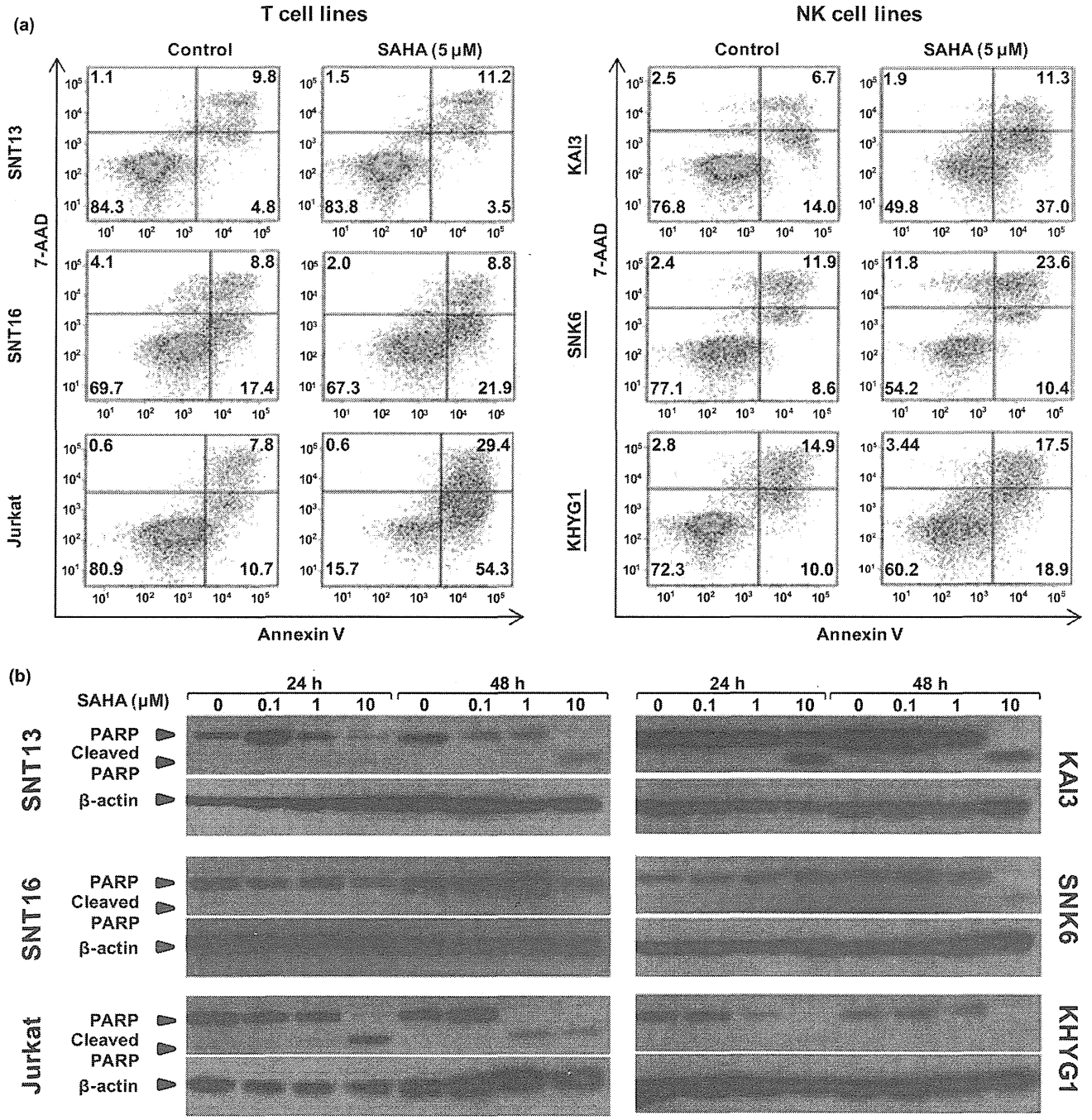

Fig. 3. Suberoylanilide hydroxamic acid (SAHA) induces apoptosis in several T and natural killer (NK) cell lines. (a) Epstein–Barr virus (EBV)-positive and EBV-negative T and NK cell lines were treated with 5 μM SAHA for 24 h. Viable cells were defined as those negative for both annexin V-PE and 7-AAD staining, and early apoptotic cells were defined as those positive for annexin V-PE but negative for 7-AAD staining. (b) T and NK cell lines were treated with the indicated concentrations of SAHA for 24 or 48 h. The cleavage of poly (ADP-ribose) polymerase (PARP) was detected by immunoblotting. β-Actin was used as a loading control.

tolerated SAHA without showing any obvious toxicity. During this period, no significant difference in the body weights of SAHA-treated and control mice was noted (data not shown). Until the end of the experiment, the size of tumors in SAHA-treated mice increased gradually, but the tumor volume was significantly less than the control group (Fig. 7a). EBER ISH showed the extent of the tumor in each mouse (Fig. 7b). In the SAHA-treated mouse, the tumor was regressed with degeneration. Additionally, SAHA-treated mice showed a significantly lower plasma EBV-DNA level (Fig. 7c). Furthermore, SAHA showed significant inhibitory effects on most EBV-encoded genes in tumor tissues (Fig. 7d). Finally, we collected samples from organs at 30 days after inoculation and performed EBER ISH. EBER-positive cells were detected in the organs of control mice, but not SAHA-treated mice (Fig. 7e). In the spleen, liver and lung, EBER-positive cells were sporadically

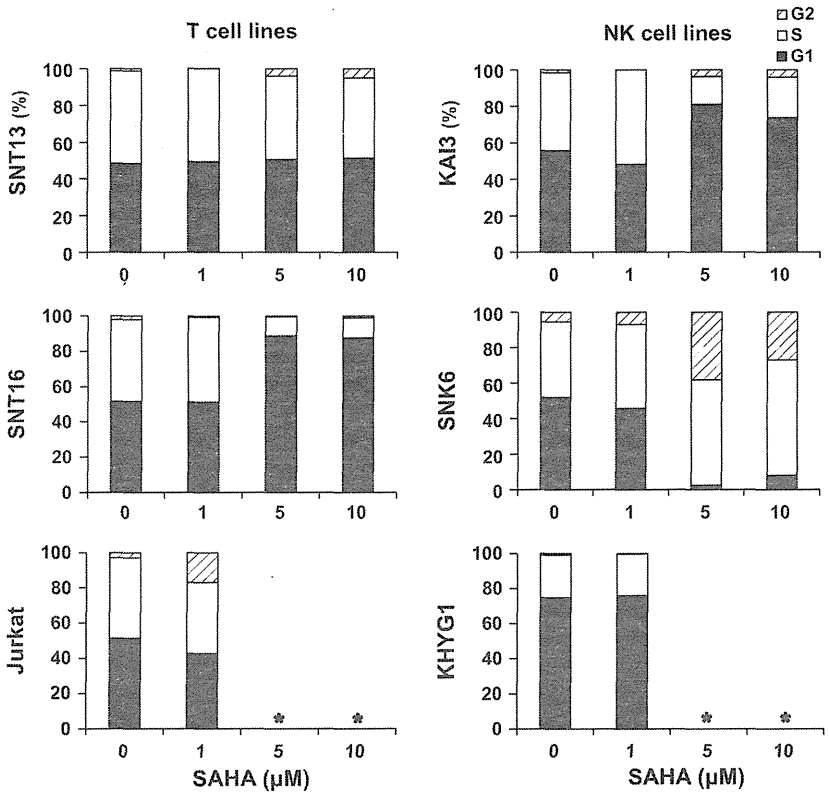

Fig. 4. Suberoylanilide hydroxamic acid (SAHA) arrests the cell cycle in T and natural killer (NK) cell lines. After treatment with the indicated concentrations of SAHA for 48 h, T and NK cell lines were fixed and stained with propidium iodide. Cell cycle profiles were assessed by flow cytometry. *Because of cell death, the cell cycle assay was indeterminable.

observed in focal lesions, indicating hematogenous dissemination of tumor cells. Conversely, the expansion of EBER-positive cells from the renal capsule to parenchyma was observed in the kidney, indicating direct invasion. These results indicated that SAHA inhibited metastasis and invasion of lymphoma cells.

Discussion

Histone deacetylase inhibitors affect tumor cell growth and survival through the induction of cell death by their characteristics of apoptosis.[6] By the upregulation of CDKNIA, HDAC inhibitors induce cell cycle arrest at the G1/S-phase. Moreover, through elongation of G2-phase, HDAC inhibitors can mediate G2/M-phase arrest, but this event occurs less frequently than G1 arrest. HDAC inhibitors can also reduce the expression of proangiogenic factors, resulting in the suppression of angiogenesis. Furthermore, HDAC inhibitors show immunomodulatory effects, which enhance tumor cell antigenicity and alter the expression of key cytokines, such as tumor necrosis factor-α, interleukin-1 and interferon-γ.[6] In the present study, SAHA markedly suppressed the proliferation of T and NK lymphoma cell lines, irrespective of the presence of EBV. The suppressive effect of SAHA was greater than that of valproic acid as demonstrated in our previous study.[8] In several T and NK cell lines, SAHA-induced apoptosis was confirmed by the increase in annexin V-positive cells and cleavage of PARP. SAHA also induced cell cycle arrest in several T and NK cell lines. The mechanism of killing appeared to differ among the cell lines. A recent study by Karube *et al.*[15] shows that suppression of the JAK-STAT pathway contributes to the suppressive effect of SAHA against NK cell lymphoma cells. Given the pleiotropic biological effects of HDAC inhibitors, it is unlikely that a single molecular pathway leading to tumor cell death will be identified in all cell types.[6]

Suberoylanilide hydroxamic acid has been reported to induce EBV lytic infection in EBV-positive gastric and nasopharyngeal carcinoma cells.[13,14] For the treatment of EBV-associated malignant diseases, induction of lytic infection is advantageous because it causes lysis of EBV-infected tumor cells. Furthermore, lytic infection should produce viral proteins with antigenicity that could induce host cellular responses. BZLF1 is an immediate-early gene and a hallmark to switch from latent gene to lytic infection.[37] In the present study, SAHA increased the expression of BZLF1 in most EBV-positive T and NK cell lines, although the late lytic gene gp350/220 was increased in only one cell line. The lytic infection induced by SAHA may play a role in its effects on EBV-infected T and NK cells. Interestingly, BZLF1, which was not expressed in the SNK-6 cell line *in vitro*, was expressed in the SNK6-derived tumor from both control and SAHA-treated mice. We speculate that the expression of BZLF1was induced in *in vivo* culture conditions presumably by nutrients or cytokines, although there is no direct poof of this.

In the present study, SAHA decreased the expression of the LMP1 gene and protein in some EBV-positive T and NK cell lines. LMP1 is a major oncoprotein that is responsible for the immortalization of primary human B lymphocytes and activation of the NF-κB, PI3K and JNK pathways.[38] Expression of LMP1 induces several pleiotropic effects, including the upregulation of adhesion molecules, anti-apoptotic proteins and cytokines. Recently, we showed that heat shock protein 90 inhibitors repress the LMP1 expression and proliferation of EBV-positive NK cell lymphoma.[35] SAHA also decreased the expression of EBNA1 in all of the cell lines. EBNA1 is essential for the maintenance of the viral episome, as well as for the initiation of latent viral replication.[38] EBNA1 also